

Integrating the Holocene tephrostratigraphy for East Asia using a high-resolution cryptotephra study from Lake Suigetsu (SG14 core), central Japan

Danielle McLean^{*a}, Paul G Albert^a, Takeshi Nakagawa^b, Takehiko Suzuki^c, Richard A Staff^{a,d}, Keitaro Yamada^e, Ikuko Kitaba^b, Tsuyoshi Haraguchi^f, Junko Kitagawa^g, SG14 Project Members^h, Victoria C Smith^a

^a *Research Laboratory for Archaeology and the History of Art, University of Oxford, Oxford, OX1 3TG, UK*

^b *Research Centre for Palaeoclimatology, Ritsumeikan University, Kyoto, 603-8577, Japan*

^c *Department of Geography, Tokyo Metropolitan University, Tokyo, 192-0397, Japan*

^d *Scottish Universities Environmental Research Centre, University of Glasgow, East Kilbride, G75 0QF, UK*

^e *Institute for Geothermal Sciences, Kyoto University, Kusatsu, 525-8577, Japan*

^f *Osaka City University, Osaka, 558-8585, Japan*

^g *Fukui Prefectural Satoyama-Satoumi Research Institute, Wakasa, 919-1331 Japan*

^h *www.suigetsu.org*

^{*}Corresponding author. *Email address:* danielle.mclean@jesus.ox.ac.uk (D. McLean)

Reference: McLean, D., Albert, P. G., Nakagawa, T., Suzuki, T., Staff, R. A., Yamada, K., Kitaba, I., Haraguchi, T., Kitagawa, J., SG14 Project Members. and Smith, V. C. 2018. Integrating the Holocene tephrostratigraphy for East Asia using a high-resolution cryptotephra study from Lake Suigetsu (SG14 core), central Japan. *Quaternary Science Reviews*, 138: 36-58. doi.org/10.1016/j.quascirev.2017.12.013

Keywords: Tephrochronology, Cryptotephra, Lake Suigetsu, Japan, Eastern Asia, Changbaishan, Ulleungdo, Holocene, Palaeoclimatology, Lacustrine

Highlights:

- *First detailed Holocene cryptotephra study in a productive volcanic arc setting*
- *Integrated Holocene tephrostratigraphic record of key East Asian isochrons*
- *Improved chronology of many widespread Holocene tephra layers*
- *New constraints on volcanism from back-arc volcanoes (Changbaishan & Ulleungdo)*
- *Reveals isochrons that can be used to synchronise to the SG14 record*

Abstract

Tephra (volcanic ash) layers have the potential to synchronise disparate palaeoenvironmental archives on regional to hemispheric scales. Highly productive arc regions, like those in East Asia, offer a considerable number of widespread isochrons, but before records can be confidently correlated using these layers, a refined and integrated framework of these eruptive events is required. Here we present the first high-resolution Holocene cryptotephra study in East Asia, using the Lake Suigetsu sedimentary archive in central Japan. The Holocene tephrostratigraphy has been extended from four to twenty ash layers using cryptotephra extraction techniques, which integrates the deposits from explosive eruptions from North Korea/China, South Korea and along the Japanese arc. This Lake Suigetsu tephrostratigraphy is now the most comprehensive record of East Asian volcanism, and the linchpin site for correlating sequences across this region. Major element glass geochemical compositions are presented for the tephra layers in the sequence, which have been compared to proximal datasets to correlate them to their volcanic source and specific eruptions. This study has significantly extended the ash dispersal of many key Holocene marker layers, and has identified the first distal occurrence of isochrons from Ulleungdo and Changbaishan volcanoes. Utilising the high-precision Lake Suigetsu chronology, we are able to provide constrained eruption ages for the tephra layers, which can be transferred into other site-specific age models containing these markers. This new framework indicates that several isochrons stratigraphically bracket abrupt climate intervals in Japan, and could be used to precisely assess the regional and hemispheric synchronicity of these events.

1. Introduction

The importance of palaeoenvironmental archives for our understanding of abrupt climate change is well recognised, but it is essential that these records can be precisely integrated and dated to assess their ultimate drivers operating across large regional scales (e.g., the East Asian Monsoon; EAM). Widely dispersed volcanic ash (tephra) layers preserved in

sedimentary sequences can provide ideal isochronous markers to facilitate high-precision correlations (tephrostratigraphy) and transfer absolute ages (tephrochronology) across palaeoclimate records (e.g., Albert *et al.*, 2013; Lane *et al.*, 2014; Abbott *et al.*, 2016; Alloway *et al.*, 2017). These markers can facilitate the assessment of the spatio-temporal variability of abrupt climate change, particularly when they bracket the onset or duration of these events (e.g., Lane *et al.*, 2013). Deciphering the regional and global synchronicity of these changes is fundamental for our understanding of the forcing mechanisms and interplay between large-scale oceanic and atmospheric systems.

In order to integrate and compare palaeoenvironmental records, regional tephrostratigraphic frameworks are established, which connect sites using widespread, and well-characterised marker layers (e.g., Shane *et al.*, 2006; Davies *et al.*, 2014; Lowe *et al.*, 2015). These regional frameworks are underpinned by key reference sites (often termed *tephrostratotypes*), which offer both detailed tephrostratigraphic sequences, and a precise chronology of eruptive events, usually from a range of volcanic sources (e.g., the Greenland ice cores; Abbott and Davies, 2012; Bourne *et al.*, 2015). Both the number and geographical footprint of these visible ash layers can be significantly extended by examining sedimentary successions for the presence of non-visible (cryptotephra) ash layers (e.g., Wastegard, 2002; Lane *et al.*, 2015; Albert *et al.*, 2015; Mackay *et al.*, 2016), which are essential to identify smaller magnitude and/or more distal occurrences of the largest eruptions.

Pioneering investigations by researchers such as Machida and Arai (1983) provide the foundation for Japanese tephrochronology, and have established a complex catalogue (via detailed mapping of visible ash deposits) of the succession and dispersal characteristics of the large explosive eruptions that occurred during the Quaternary (compiled in Machida and Arai, 2003). In other parts of the world, studies like those undertaken by the RESET ('Response of Human to Abrupt Environmental Transitions') project, centred in continental Europe and across the Mediterranean Sea (see Lowe *et al.*, 2015), have further refined tephrostratigraphic frameworks through detailed analysis of key eruption sequences and at distal sites. In the RESET project, all tephra deposits were sampled and geochemically

fingerprinted from proximal eruptive units close to their source, and detailed cryptotephra studies were undertaken in distal sedimentary sequences. These analyses were able to: i) incorporate new and lower magnitude events into the master European tephrostratigraphic framework (e.g., Albert *et al.*, 2013), ii) resolve the stratigraphic position of eruptions from different volcanic sources that were closely spaced in time (e.g., Karkanias *et al.*, 2015), iii) establish which eruptions have a diagnostic geochemical signature for reliable tephra correlations (e.g., Smith *et al.*, 2011a), (iv) identify erroneous tephra correlations (e.g., Albert *et al.*, 2015), and v) extend the known geographical footprint of ash fallout from individual eruptions, and therefore widen the area over which the key isochrons could be used. This detailed work has revised and verified a comprehensive framework (Lowe *et al.*, 2015) that can be used to robustly integrate key palaeoenvironmental and archaeological archives across the region surrounding the Mediterranean Sea, and test long-standing questions using the high-resolution chronology (e.g., Rohling *et al.*, 2009; Grant *et al.*, 2012; Lowe *et al.*, 2012; Barton *et al.*, 2015).

This project aimed to refine and augment the Holocene tephrostratigraphic framework for the East Asian/Pacific region using a similar methodology to that employed by the RESET project (outlined above). Here, the sediments of Lake Suigetsu (SG14 core; Figure 1) were targeted for detailed cryptotephra analysis, since it currently provides the most precisely dated Holocene sedimentary record from Japan (see Nakagawa *et al.*, 2012; Staff *et al.*, 2011). The objectives of this research were to: i) verify the successful application of cryptotephra analysis from a lake located along the highly productive volcanic arc, ii) chemically characterise and date identified tephra isochrons in order to correlate them to their volcanic source and, where possible, specific eruptions, and iii) use the Holocene tephrostratigraphic record from Lake Suigetsu to develop an integrated framework for the East Asian/Pacific region.

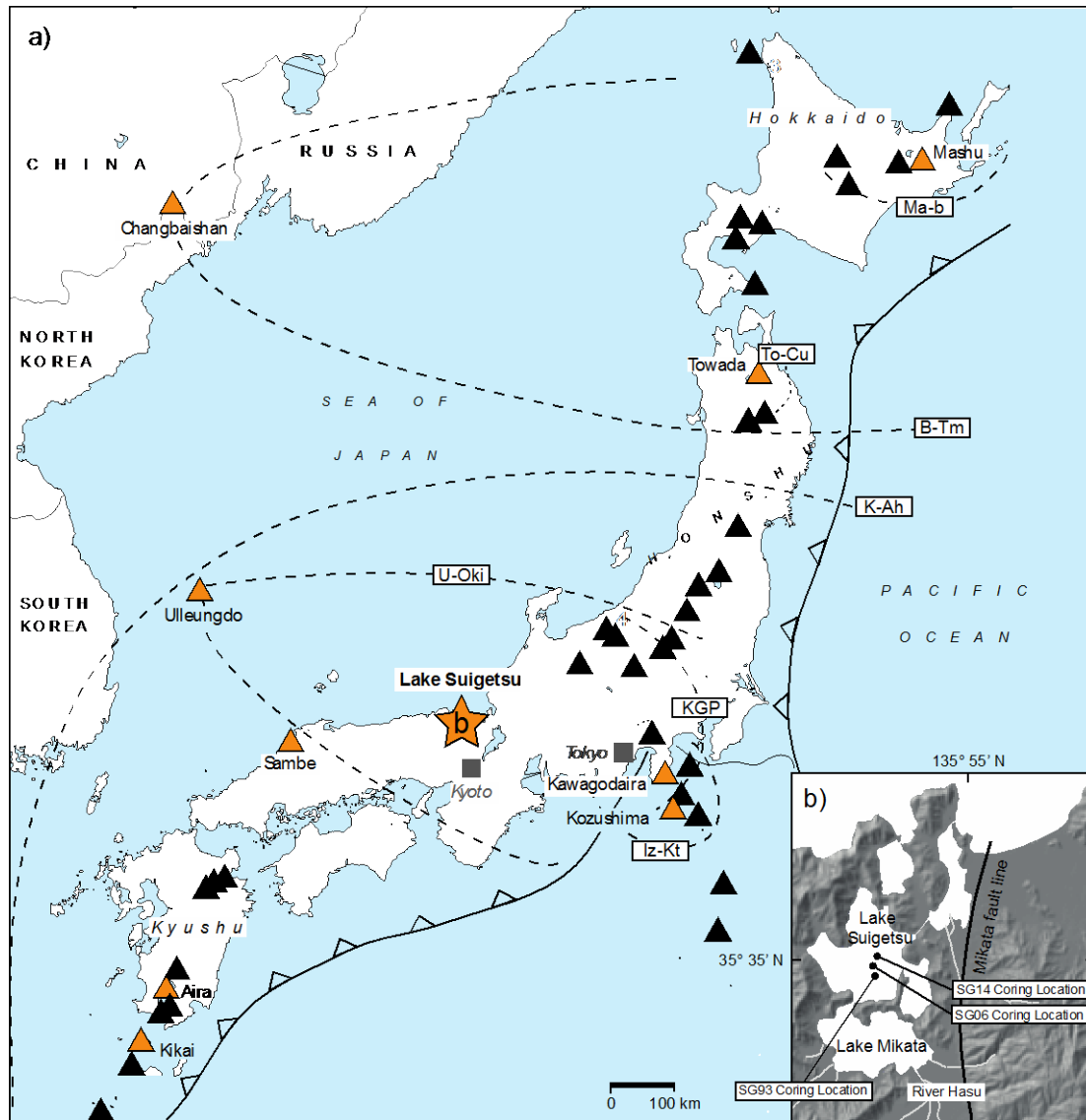


Figure 1: (a) Volcanoes in Japan, North Korea/China (Changbaishan volcano) and South Korea (Ulleungdo volcano) known to have been active during the Holocene (data obtained from VOGRIPA, 2016). Large caldera volcanoes in Japan, which are the sources of the most explosive eruptions, are concentrated on the island of Kyushu (south) and Hokkaido (north). Volcanoes mentioned within the text are coloured orange, and a star denotes the location of Lake Suigetsu. Dispersal boundaries (dashed lines) are shown for Holocene visible tephra layers (white boxes) Ma-b (Mashu volcano), B-Tm (Changbaishan), Iz-Kt (Kozushima), KGP (Kawagodaira), To-Cu (<10 cm isopach, Towada), K-Ah (Kikai) and U-Oki (Ulleungdo), as mapped by Machida and Arai, 1983. (b) Location of the five Mikata lakes, including the study site Lake Suigetsu, which are situated west of the Mikata fault line. The positions of coring campaigns SG93, SG06 and SG14 are also marked on Lake Suigetsu (modified after Nakagawa *et al.*, 2005).

1.1. Tephra dispersal in and around Japan

Over 130 volcanic centres are distributed along the length of the Japanese arc (Figure 1). These centres have been highly productive during the Late Quaternary, with numerous large caldera-forming eruptions (particularly on Hokkaido and the Kyushu Islands; Figure 1) producing widespread tephra dispersal across the East Asian/Pacific region (Machida and Arai, 2003). Due to the prevailing westerly winds, ash from the explosive back-arc volcanism in South Korea (Ulleungdo volcano) and North Korea/China (Changbaishan) has also blanketed Japan and the surrounding seas numerous times over the Quaternary (Machida and Arai, 2003; Lim *et al.*, 2013; Figure 1).

During the Holocene three key widespread marker beds are commonly identified in sedimentary sequences in and around Japan, and are named using their source volcano and distal tephra type-site, a common practise in Japanese tephrostratigraphy studies. These include the Baegdusan-Tomakomai (B-Tm), Kikai-Akahoya (K-Ah) and Ulleungdo-Okii (U-Okii) ash (Machida and Arai, 1983). The B-Tm is the tephra deposit from the 'Millennium' eruption of Changbaishan, and has been recently dated to AD 946 (Oppenheimer *et al.*, 2017; Hakoizaki *et al.*, 2017). The K-Ah tephra was dispersed from the now largely sub-marine Kikai caldera, located 50 km south of Kyushu. The most precise date for this eruption (7303 – 7165 cal. yrs BP), was obtained from the Lake Suigetsu SG06 sediment core (Smith *et al.*, 2013). The U-Okii tephra is from Ulleungdo Island (South Korea), which is located in the Sea of Japan, and corresponds to the U-4 proximal eruptive unit (Smith *et al.*, 2011b). Lake Suigetsu, situated in central Japan, is the only archive to currently record all three of these key Holocene marker beds (Figure 1; Smith *et al.*, 2011b; Smith *et al.*, 2013; McLean *et al.*, 2016).

In the past, the majority of tephra correlations in and around Japan are based on the physical characteristics of the deposit, i.e. refractive indices, layer thickness, grain-size and modal mineralogy. However, it is essential that tephra layers are geochemically characterised as accurately as possible to ensure unequivocal correlations across the proximal and distal

settings. Volcanic glass compositions are routinely employed for robust tephra correlation around the world, including New Zealand (e.g., Froggat, 1983; Shane and Smith, 2000) Europe (e.g., Tomlinson *et al.*, 2015), North America (e.g. Smith and Westgate, 1968; Sarna-Wojcicki *et al.*, 1987) and South America (e.g. Fontijn *et al.*, 2016), but are only recently being utilised in Japan (e.g. Moriwaki *et al.*, 2011; Okuno *et al.*, 2011; Smith *et al.*, 2013; Chen *et al.*, 2016). Comprehensive glass datasets are yet to be obtained from many eruptive centres in this region, particularly those in central and southern Japan, which means that many distal correlations remain unconfirmed (e.g. Smith *et al.*, 2013).

1.2. Constraining Holocene climate intervals using tephra layers

Palaeoenvironmental change during the Holocene can provide an improved perspective upon the causal mechanisms and drivers of climate change across the globe (Wanner *et al.*, 2008). In the East Asian/Pacific region, the Holocene climate has been shown to vary considerably, with several abrupt (centennial-scale) warming and cooling phases, likely caused by fluctuations in the behaviour of the East Asian Monsoon (EAM; Wang *et al.*, 2005; Sagawa *et al.*, 2014; Tada and Murray, 2016). Despite the regional and global importance of this climate system, its causal relationship to both external (e.g., orbital, solar and volcanic) and internal forcing remains poorly understood (Morrill *et al.*, 2002; Park, 2017). This is partly due to the inherent difficulties in precisely comparing the distant and diverse palaeoclimate archives across the monsoon region.

Tephra layers can be used to precisely integrate disparate palaeoenvironmental records across the migration paths of the EAM, and develop a more comprehensive picture of the spatio-temporal changes of this system. Visible ash layers are commonly recognised in key marine (e.g., Furuta *et al.*, 1986; Park *et al.*, 2003; Sagawa *et al.*, 2014; Chun *et al.*, 2007; Aoki *et al.*, 2008; Ikehara *et al.*, 2011) and terrestrial (e.g., Domitsu *et al.*, 2002; Kumon *et al.*, 2003; Nagahashi *et al.*, 2004; Okuno *et al.*, 2011; Smith *et al.*, 2013) sedimentary archives across this region, but very few have thus far been detected over wide areas, prohibiting the synchronisation of these records, and few are adequately dated to improve site-specific age

models. No detailed cryptotephra investigations have been undertaken to explore the true dispersal potential of key ash layers in Japan, however tephra from East Asia has been transported and deposited as isochrons across the northern hemisphere, with recent discoveries in the Greenland ice cores (Sun *et al.*, 2015a; Bourne *et al.* 2016), and possibly as far as the North American east coast (Mackay *et al.*, 2016). This provides substantial encouragement that additional cryptotephra investigations in the East Asian/Pacific region will resolve new isochrons suitable for regional and hemispheric-scale correlations.

2. Study site

2.1. Lake Suigetsu sediment record

The Lake Suigetsu sedimentary archive, central Japan (Figure 1) has numerous characteristics that make it suitable for detailed cryptotephra analysis and to provide a comprehensive Holocene tephrostratigraphic framework for the East Asian/Pacific region.

1. The visible tephrostratigraphic record (spanning ~150 ka) confirms that the lake is ideally situated to record explosive eruptions from multiple volcanic sources from across Japan, South Korea and North Korea/China (Smith *et al.*, 2011b; Smith *et al.*, 2013; McLean *et al.*, 2016).
2. Suigetsu is a tectonic lake, adequately situated away from the large calderas in Hokkaido and Kyushu, so is unlikely to be inundated with locally sourced volcanic products (i.e. background glasses) that could obscure the cryptotephra record.
3. No rivers flow directly into Lake Suigetsu, which mean that the basal sediments are rarely disturbed by inflows from the immediate lake surroundings. The sedimentation is relatively fast with the accumulation of ~12 m of fine-grained sediment through the Holocene (Nakagawa *et al.*, 2012; Yamada *et al.*, submitted), which is ideal for high-resolution tephra investigations and palaeoenvironmental proxy analysis.
4. A detailed Bayesian age-model has been generated for the Holocene section of the sediment sequence (Staff *et al.*, 2011; Yamada *et al.*, submitted) from a high-resolution radiocarbon dataset (124 measurements of terrestrial plant macrofossil

remains), and provides precise and well-constrained age estimates for identified eruption events. Since the Holocene sediments do not contain visible varves and the chronology is reliant on the ^{14}C dating, identifying precisely dated tephra layers can help improve the Lake Suigetsu chronology at their respective depths.

5. The lake is located in the mid-latitude western Pacific region where the EAM front annually migrates, and thus records the past behaviour of this sensitive climate system.
6. The archive is a key global palaeoenvironmental record (e.g., Nakagawa *et al.*, 2005; Nakagawa *et al.*, 2012), with the lake currently recognised as an auxiliary stratotype for the onset of the Holocene (Walker *et al.*, 2009).

2.2. Geology of the Lake Suigetsu catchment

Lake Suigetsu, Honshu Island (35°35'0"N, 135°53'0"E) is located in a small tectonic basin situated on the western side of the Mikata fault line, adjacent to Wakasa Bay (Figure 1). It forms the largest of the 'Mikata Five Lakes' and is located in the Wakasa Wan Quasi-National Park. Lake Suigetsu covers an area of ~4.3 km² (with a perimeter of ~10 km and diameter of ~2 km) and has an average water depth of ~34 m (Kitagawa and van der Plicht, 1998a).

The lake has a small catchment area that is vegetated by warm mixed-forest and is surrounded by a ring of Palaeozoic hills (maximum elevation 400 m) (Kitagawa *et al.*, 1995; Nakagawa *et al.*, 2005). The main tributary feeding the five Mikata lakes is the River Hasu (~10 km in length), which enters on the southeast side of Lake Mikata (Figure 1b). Water subsequently flows through the Seto Channel into Lake Suigetsu. This channel is particularly shallow (~2 m in depth), meaning coarse sediment is deposited or trapped in Lake Mikata before reaching Lake Suigetsu (Nakagawa *et al.*, 2005). This natural filter, means that sediments entering Lake Suigetsu are predominantly comprise of autochthonous and authigenic material (Schlölaut *et al.*, 2012). These sediment characteristics and the geomorphic protection of the lake mean the sedimentary environment is particularly stable and allows for continuous fine-grain deposition.

2.3. Coring campaigns

The Suigetsu lake sediments have been studied for over two decades, with significant interest sparking with the 1993 'SG93' campaign, which obtained a 72.4 m piston core from the basal lake sediments (Kitagawa and van der Plicht, 1998a). This revealed that much of the sequence contained varves (*'nenko'* in Japanese) i.e. seasonal laminations, with alternations of diatom-rich (darker coloured) and mineral-rich (lighter coloured) layers (Fukusawa, 1995; Kitagawa *et al.*, 1995; Kitagawa and Van der Plicht, 1998a). The lake was re-drilled in the summer of 2006 as part of the 'Lake Suigetsu Varved Sediment Project' with the aim of obtaining a complete overlapping 'master' sedimentary sequence by recovering overlapping cores from four parallel boreholes (A, B, C and D, situated ~20 m apart; Figure 1b) (see Nakagawa *et al.*, 2012). This coring campaign successfully obtained a 73.19 m-long composite core ('SG06'), providing a continuous record of sedimentation spanning the last ~150 ka (Nakagawa *et al.*, 2012). The sequence has been extensively radiocarbon (^{14}C) dated and is varved between ~10 and 70 ka, which provides a very high-resolution chronology for this palaeoenvironmental record (Staff *et al.*, 2011; Bronk Ramsey *et al.*, 2012; Marshall *et al.*, 2012 and Schlolaut *et al.*, 2012).

A new coring campaign was undertaken during the summer of 2014 to obtain another continuous core sequence to: i) generate thin-sections for a display at a purpose-built Lake Suigetsu museum, and ii) provide more material for scientific analysis (see Yamada *et al.*, submitted). The coring site was located ~320 m east of the SG06 boreholes (Figure 1b) and was similarly obtained using a hydro-pressure piston sampler, and also a triple sampler for deeper parts. This campaign retrieved a composite overlapping sedimentary sequence again from four boreholes (E, F, G and H) and it spans ~98 m, which records ~25 m of extra sedimentation compared to SG06, reaching a thick basal gravel. This composite master sequence, named 'Fukui-SG14' ('SG14' in short), was used for this Holocene cryptotephra investigation. The SG14 sequence (correlation model 30 May '17) has been precisely tied to the SG06 composite core (correlation model 08 May '16) using 361 common marker layers

(which include visible tephra layers), permitting the high-precision SG06 chronology to be transferred to the SG14 core (see Yamada *et al.*, submitted).

2.4. Lake Suigetsu tephrostratigraphy

Hitherto, 31 visible tephra layers from SG06 have been identified and characterised (using major element geochemical analysis), providing a detailed record of East Asian eruption events over the past 150 ka (Smith *et al.*, 2011b; Smith *et al.*, 2013; McLean *et al.*, 2016). These include some of the most widespread tephra layers from southern Japan and South Korea, including the B-Tm, K-Ah, U-Oki, AT, Aso-4, K-Tz, Aso-ABCD and Ata tephra layers.

Four visible layers were identified from the Holocene section of the SG06 sediments. These include the following tephra layers: SG06-1288 that has been correlated to the U-Oki (U-4) eruption; SG06-0967 which has been correlated to the K-Ah tephra; SG06-0588 from an unknown eruption source; and SG06-0226 that is correlated to the B-Tm tephra (Smith *et al.*, 2011b; Smith *et al.*, 2013; McLean *et al.*, 2016). During the 2014 coring campaign, several new visible tephra layers were identified (Yamada *et al.*, submitted), including two in the Holocene sediments (SG14-1091 and SG14-0781) that are characterised and dated herein.

3. Materials and methods

3.1. Tephra identification

The master SG14 core (composite sequence) was contiguously sub-sampled at a ~5 cm resolution, from the U-Oki tephra to the core top, avoiding the known high-energy event layers (e.g., flood horizons) defined by Yamada *et al.*, (submitted) (see Section 4.1). If elevated shard concentrations were observed in the ~5 cm sample, the sediment was resampled at a 1 cm resolution to determine the precise stratigraphic positioning of the peak. All samples were wet sieved through a 25 µm mesh, and processed using the heavy liquid floatation method outlined by Turney (1998) and Blockley *et al.*, (2005). These samples were

prepared alongside blanks to test for possible laboratory contamination. The extraction residues were mounted on slides using Canada Balsam, and glass shards were counted via microscopic examination to quantify the number of shards per gram of dried sediment (shards/gram). The following characteristics were also recorded for the glass shards (Figure 2):

- (i) Colour (e.g., clear, brown or green)
- (ii) Size (length of the longest axis of shards in the fraction extracted, i.e. >25 microns)
- (iii) Morphology (e.g., blocky, platy, cusate or fluted)
- (iv) Vesicle size (small/microvesicular or large) and density (rich or poor)
- (v) Microlite density (rich or poor)

3.2. Glass geochemical analysis

Glass shards were extracted from samples chosen for geochemical analysis and hand-picked from a well-slide using a micromanipulator (see Lane *et al.*, 2014). These shards were mounted in Epoxy resin stubs, which were sectioned and polished to expose a flat surface, and carbon coated for chemical analysis. Major and minor element compositions of individual glass shards were measured using a JEOL-8600 wavelength-dispersive electron microprobe (WDS-EMP) at the Research Laboratory for Archaeology and History of Art (RLAHA), University of Oxford. All analyses used an accelerating voltage of 15 kV, beam current of 6 nA and 10 µm-diameter beam. Peak counting times were 12 s for Na, 50 s for Cl, 60 s for P, and for 30 s for all other elements. The electron microprobe was calibrated using a suite of mineral standards, and the PAP absorption correction method was applied for quantification. The accuracy and precision of this data were assessed using analyses of the MPI-DING reference glasses (Jochum *et al.*, 2006), which were run as secondary standards during all runs of the Lake Suigetsu tephra samples. Analyses of these secondary standards lie within a standard deviation of the preferred values. Data were filtered to remove non-glass analyses, and those with analytical totals < 93%. The raw values were normalised (to 100 %) for

comparative purposes and to account for variable hydration, and are presented as such in all tables and figures.

General Morphology

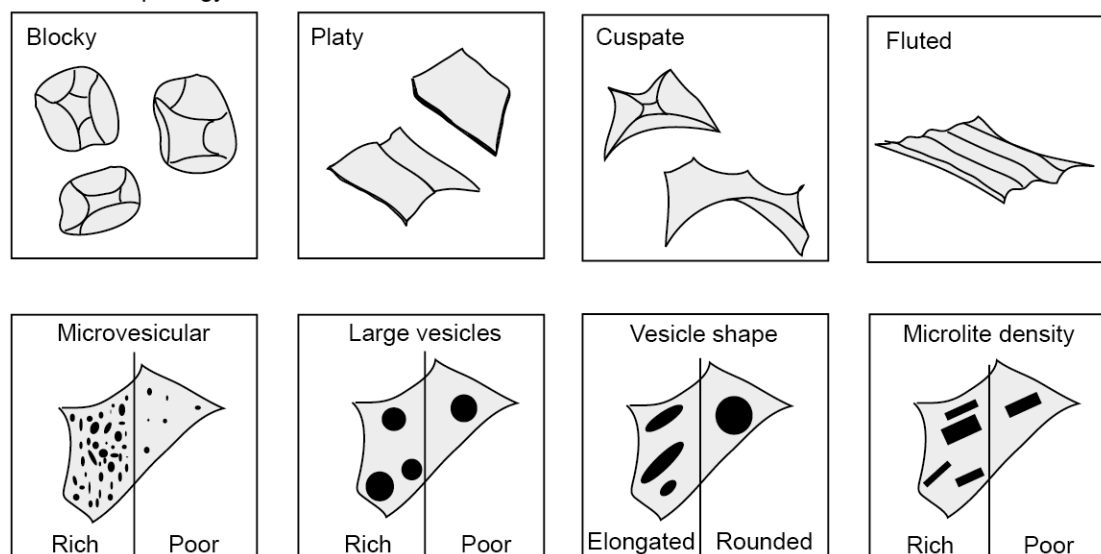


Figure 2: Schematic representation of the end member glass morphologies observed in the Lake Suigetsu sequence. Glass shards from an individual layer (i.e. primary isochron) typically possess a uniform shard size and consistent morphology. Glass shards which are both blocky and microvesicular are referred to as pumiceous.

Proximal glass data from several eruptive units at Mashu, Towada and Kawagodaira volcanoes were analysed using the same procedure to validate tephra correlations. Details of these sampling localities and glass datasets are provided in the Supplementary Material.

3.3. Chronology

As introduced above, the master SG14 sequence was precisely tied to SG06, permitting the high-precision SG06 chronology to be transferred to the SG14 core. SG06 event-free depth(s) (EFD, ver. 29th Jan '11) were used within the age model, which excludes instantaneous deposits > 5 mm in thickness, i.e. event layers, e.g., floods, and tephra deposits (Staff *et al.*, 2011; Scholaut *et al.*, 2012). The software package developed to handle the correlation of parallel core sections, 'LevelFinder' (ver. 7.5.5, <http://polsyems.rits-palaeo.com>), was used to linearly extrapolate between the common marker layers and

determine any given composite depth (CD) or EFD from the individual SG06 and SG14 cores (see Nakagawa *et al.*, 2012; Yamada *et al.*, submitted).

The composite Suigetsu sedimentary sequence was modelled on to the IntCal13 timescale (Reimer *et al.*, 2013) implementing three successive cross-referenced Poisson-process ('*P_Sequence*') depositional models using OxCal (ver. 4.3; Bronk Ramsey 2008; 2017). These include 775 AMS ^{14}C dates obtained from terrestrial plant macrofossils from the upper 38 m (SG06-CD) of the SG93 and SG06 cores (Kitagawa and van der Plicht, 1998a, 1998b, 2000; Staff *et al.*, 2011, 2013a, 2013b) and varve counting between 12.88 and 31.67m SG06 CD (Marshall *et al.*, 2012; Schlolaut *et al.*, 2012).

The uppermost Holocene sediments, from the core top down to the SG06-1288 (U-Okii) tephra (12.88 m SG06 CD, ~10200 cal. yrs BP), are not composed of clearly defined and countable varves, and the chronology is instead constrained by 124 ^{14}C dates. Several additional chronological constraints are incorporated within the Holocene section of the age model, including a calendar age for the Urami Canal construction (AD 1664 \pm 5 yrs positioned at 87.8 cm SG06-CD; as determined by an influx of marine diatom species into Lake Suigetsu; Saito-Kato *et al.*, 2013), a calendar age for event layer A-01-01c (AD 1976 \pm 2 positioned at 32.5 cm SG06-CD; as determined by varve counting of the uppermost sediments; Suzuki *et al.*, 2016) and a constrained age for the core top (which cannot post-date AD 2006). Three precise tephra-based ages are also included following the findings of this study (see discussion), including a remodelled tree-ring wiggle-matched ^{14}C age for the KGP tephra (3151 – 3126 cal yrs BP, 95.4% confidence interval; Tani *et al.*, 2013) imported as a '*Prior*' within the model (spanning the cryptotephra sampling interval of 484.0 – 485.0 cm SG06-CD), a historical age for the Iz-Kt eruption (AD 838; spanning the cryptotephra sampling interval 239.1 – 240.1 cm SG06-CD; Tsukui *et al.*, 2006) and a tree-ring wiggle-matched age for the B-Tm tephra (AD 946 \pm 1; Oppenheimer *et al.*, 2017) positioned at 225.5 cm SG06-CD.

Cryptotephra layers are usually inserted into age models using the sub-sampling mid-point instead of the depth range and therefore, the date may not be accurate and the precision is underestimated. In this study, we have included this cryptotephra sample depth uncertainty into our age modelling. Our results indicate that the effect on the chronology in this case is negligible, but this modelling approach should be applied in other such cryptotephra studies to account for the full age uncertainty.

4. Tephrostratigraphy Results

4.1. Discriminating primary tephra layers

When interpreting the visible and cryptotephra record, it is necessary to consider the possibility of syn- and post- depositional processes which may: i) obscure the original stratigraphic positioning of the eruption event, and ii) incorporate older or background volcanic glasses that have been reworked and redeposited in the sediments (Davies *et al.*, 2007; Pyne-O'Donnell, 2011).

Some sedimentary sequences, especially those located too close to a volcanic source, may be unsuitable for cryptotephra analysis, as they might be continuously inundated with ash. High concentrations of tephra shards are often observed following a large explosive eruption that has previously blanketed the catchment with ash, and can produce a large and persistent background of volcanic glass in the lake sediments after the event (e.g., Zawalna-Geer *et al.*, 2016; Matsu-ura *et al.*, 2017). As expected, high concentrations of glass shards are observed in the Lake Suigetsu core sediments following the visible ash layers, for example, after the ~3 cm thick K-Ah tephra (SG06-0967) distinctive platy shards were continuously observed, in excess of 5000 shards/gram, for several metres. However, these concentrations did not obscure the stratigraphic positioning of all primary ash layers deposited during this period, due to contrasting shard morphologies (e.g., peaks in cusped or vesicular glass shard populations) or colour of subsequent primary ash layers.

Other peaks in shard concentrations may not always represent in-situ or primary ash input, as shards from older eruptions may be reworked from the catchment or local geology during high-energy events (e.g., MacLeod and Davies, 2016). Such high-energy events may be caused by heavy rains or earthquakes, which can erode sediments and thus remobilise older volcanic material from the catchment. These events can usually be visually identified within the core, since they deposit a distinct detrital layer that is typically clay-rich, which contrasts to the authigenically-produced, organic-rich sediments that are commonly deposited (Katsuta *et al.*, 2007; Bussmann and Anselmetti, 2010; Swierczynski *et al.*, 2012; Corella *et al.*, 2014).

Several lines of evidence can also be used to distinguish between primary and secondary ash layers that are not accompanied by an obvious high-energy event deposit within the sediment core (Gudmundsottir *et al.*, 2011; Abbott *et al.*, 2016). A high-energy or reworking event will typically incorporate volcanic glasses from several older eruptions, meaning the shards will often contain a range of morphologies, sizes and geochemical affinities. In the Lake Suigetsu sequence peaks in shard concentrations were ultimately evaluated using a set of criteria outlined in Figure 3. Glasses from flood horizons, and other positions where shard concentrations were largely constant, were geochemically analysed to establish the background compositional range. Peaks in volcanic glass concentrations were considered to be primary tephra if the shards possessed a consistent morphology, size and geochemical affinity that was different from the known background compositions.

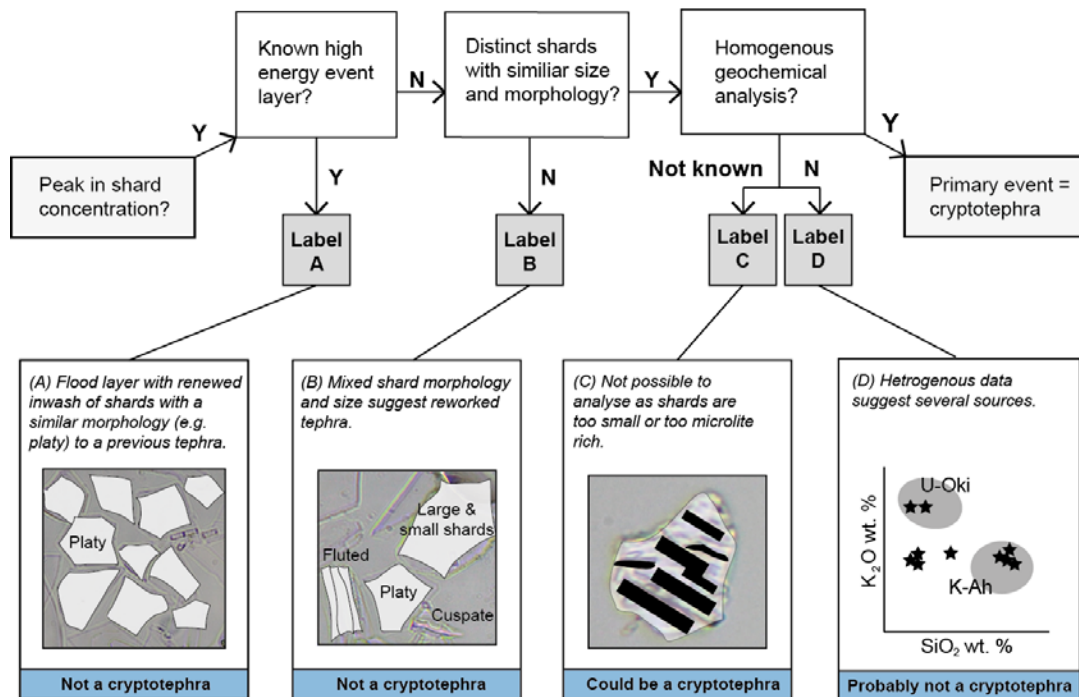


Figure 3: Criteria used to decipher primary ash fall events within the Lake Suigetsu sedimentary sequence (Y=yes, N=no). Peaks in glass concentration that fail these criteria and unlikely to reflect a primary event are marked by A, B, C or D on Figure 4.

4.2. Overview of Lake Suigetsu Holocene tephrostratigraphy

In total, twenty primary ash layers (six visible and fourteen cryptotephra layers) were identified within the Lake Suigetsu SG14 core (Figure 4; Figure 5; Table 1). Newly identified ash layers are herein labelled using their SG14 composite depth in cm (SG14-CD, correlation model 30 May '17) that is rounded to the nearest integer. For continuity, SG06 codes are used for the visible tephra layers that were previously identified in the Holocene sections of the SG06 core; SG06-1288 (U-Oki ash), SG06-0967 (K-Ah ash) SG06-0588 and SG06-0226 (B-Tm ash) (Table 1; Smith *et al.*, 2011b; Smith *et al.*, 2013; McLean *et al.*, 2016).

The Holocene tephrostratigraphy is described in three zones for simplicity (Figure 4), and are demarcated by the variable concentrations of background glasses through the core.

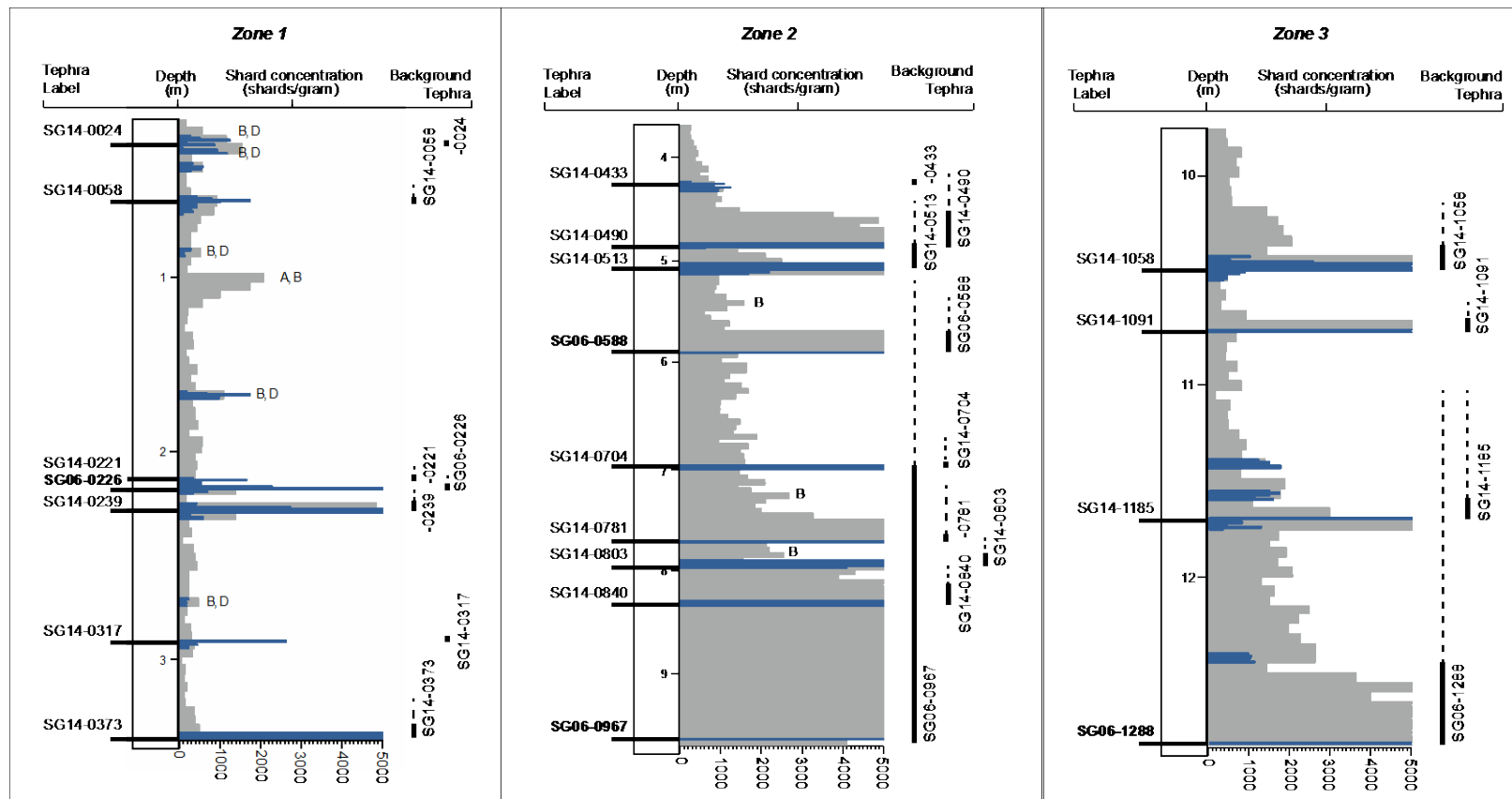


Figure 4. Glass shard concentrations (shards per gram of dry sediment; capped at 5,000) in the Holocene sediments of the Lake Suigetsu SG14 core. The tephrostratigraphy is divided into three Zones (1 to 3) for ease of description in Section 4. Concentration of low-resolution (5 cm) samples are shown in grey and high-resolution samples (1 cm) are overlain in blue. Tephra isochrons are labelled using their SG06/SG14 composite depth. Vertical bars indicate the relative concentration of, dominant (solid line) and minor (dotted line), background glasses in the section based on the typical morphology of the glass shards.

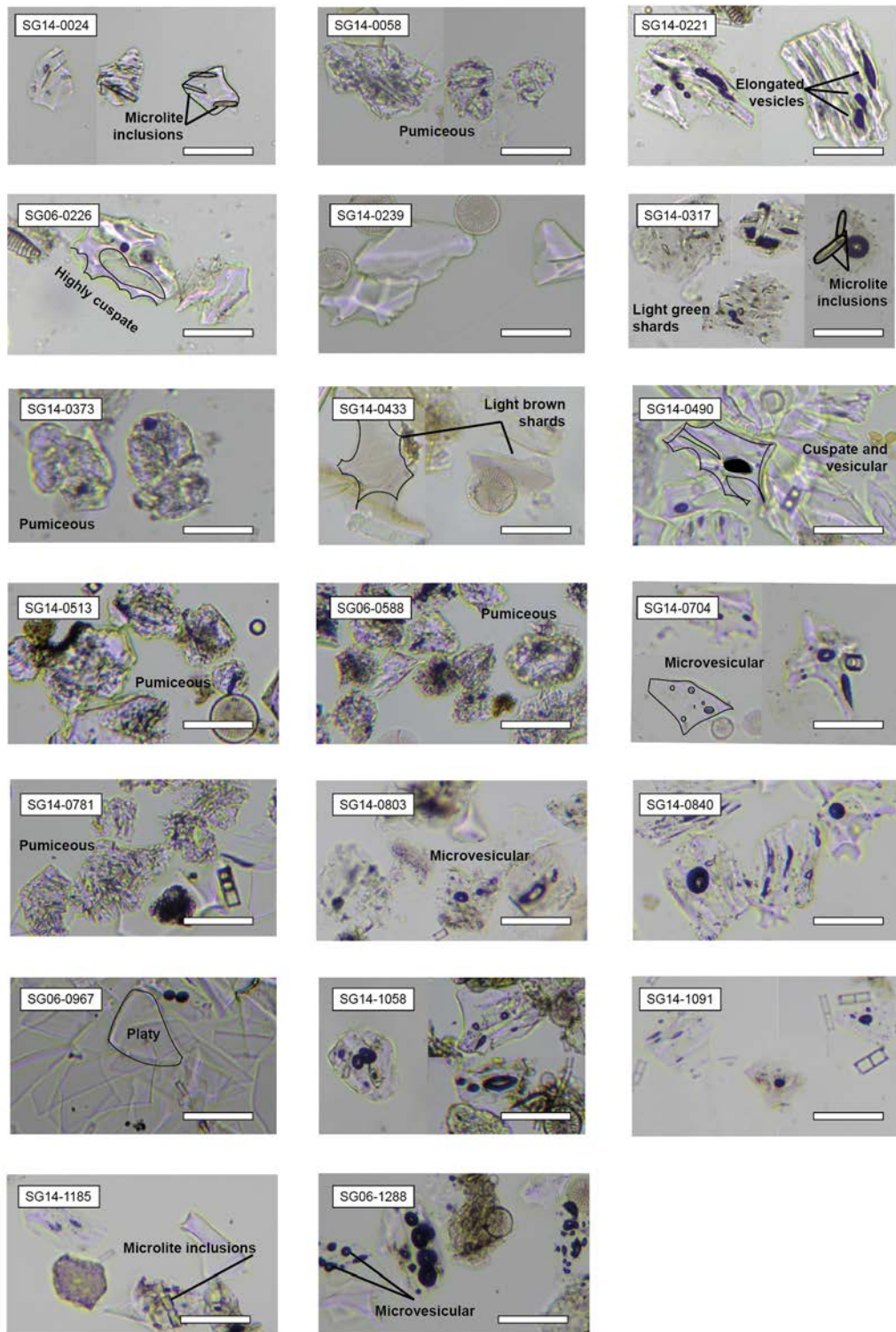


Figure 5: Photographs of the typical glass shards preserved in the SG14 Holocene tephra ash layers, scale bar = 50 μm. Morphologies vary from platy (e.g. SG06-0967), highly cusped (e.g. SG06-0226) to pumiceous (e.g. SG14-0791). Some shards morphologies are densely vesicular (e.g. SG06-11288) and/or contain microlite inclusions (e.g. SG14-0024).

Table 1: Summary table of the Holocene tephras within the Lake Suigetsu SG06 and SG14 sediment cores

Label	V/C	SG14 Master core and position *	SG14 Composite Sampling Depth (cm) *	SG06 Composite Sampling Depth (cm) *	Glass shard morphology	Shard length (µm)**	Glass compositions of dominant population (wt %)				¹⁴ C date (AD / cal. yrs BP) 95.4 % uncertainty	Correlation based on glass geochemistry (tephra, volcano)***	Distance of source volcano from Lake Suigetsu (km)	Magnitude of eruption (VEI)
							SiO ₂	K ₂ O	CaO	n				
SG14-0024	C	E-01 (15.1 - 16.0 cm)	23.3 - 24.2	39.1 - 40.0	MI	30	68.50 - 69.90	2.48 - 2.62	3.12 - 3.68	6	AD 1963 - 1920	-	-	-
SG14-0058	C	E-01 (48.9 - 49.9 cm)	57.1 - 58.1	70.6 - 71.4	PU, MV, MI	70	-	-	-	-	AD 1746 - 1902	-	-	-
SG14-0221	C	F-02 (81.0 - 82.0 cm)	219.7 - 220.7	220.5 - 221.6	C, F, V, MV	50	71.92 - 73.79	0.72 - 0.88	0.57 - 0.69	14	AD 960 - 992	Ma-b, Mashu	1160 NE	5
SG06-0226 ¹	V	F-02 (85.7)	224.4	225.5	C, V	80	65.14 - 75.49	6.15 - 4.21	0.18 - 1.42	30	AD 946 ⁴	B-Tm, Changbaishan ¹	980 NW	7
SG14-0239	C	E-03 (15.0 - 15.9 cm)	237.8 - 238.7	239.1 - 240.1	C	100	77.49 - 78.37	3.20 - 4.08	0.32 - 0.93	20	AD 767 - 839	Iz-Kt, Kozushima	340 SE	4
SG14-0317	C	F-03 (60.0 - 61.0 cm)	315.5 - 316.5	317.0 - 317.9	V, MI	40	-	-	-	-	1815 - 1735	-	-	-
SG14-0373	C	E-04 (68.1 - 69.1 cm)	372.1 - 373.1	371.3 - 372.3	PU, MV, MI	40 - 100	-	-	-	-	2192 - 2117	-	-	-
SG14-0433	C	F-04 (57.8 - 58.8 cm)	431.9 - 432.9	429.0 - 430.0	PL, C	60 - 80	61.53 - 62.00	4.48 - 4.75	2.47 - 2.72	8	2737 - 2620	U-1, Ulleungdo ?	980 NW	-
SG14-0490	C	G-02 (50.2 - 51.2 cm)	489.4 - 490.4	484.0 - 485.0	C, F, V	30 - 100	76.49 - 77.56	2.65 - 2.94	1.43 - 1.83	19	3227 - 3129	KGP, Kawagodaira	290 E	4
SG14-0513	C	G-02 (73.2 - 74.2 cm)	512.4 - 513.4	506.3 - 507.3	PU, MI	50	-	-	-	-	3428 - 3312	-	-	-
SG06-0588 ²	V	F-06-04	593.7	587.8	PU, MV, MI	30 - 70	74.40 - 77.97	2.25 - 3.99	1.45 - 2.37	11	4066 - 3986	-	-	-
SG14-0704	C	E-08 (36.0 - 37.0 cm)	703.2 - 704.2	699.1 - 700.0	C, F, V, MV	50	70.39 - 72.97	2.49 - 2.91	2.41 - 3.64	10	4894 - 4827	Unknown, Kikai ?	750 SW	-
SG14-0781	V	F-08-06	780.5	775.4	PU, MI	30 - 100	74.41 - 78.00	1.98 - 3.79	1.25 - 2.48	26	5519 - 5480	-	-	-
SG14-0803	C	E-09 (43.7 - 44.7 cm)	802.1 - 803.1	797.9 - 798.9	MV	30 - 50	59.43 - 61.76	6.26 - 7.02	1.23 - 2.49	19	5681 - 5619	U-2, Ulleungdo	500 NW	-
SG14-0840	C	E-09 (80.7 - 81.7 cm)	839.1 - 840.1	835.9 - 836.9	C, MV	40	73.43 - 74.41	1.09 - 1.31	2.60 - 3.13	25	5986 - 5899	To-Cu, Towada	700 NE	5
SG06-0967 ²	V	F-10-04	977.1	967.2	PL	50 - 100	72.60 - 74.60	2.77 - 3.03	1.82 - 2.34	14	7307 - 7196	K-Ah, Kikai ²	750 SW	7
SG14-1058	C	F-11 (28.6 - 29.4 cm)	1057.1 - 1057.9	1050.8 - 1051.6	C, F, V	50	74.54 - 75.30	4.39 - 4.60	0.17 - 0.26	25	8166 - 8099	Unknown, Changbaishan	980 NW	-
SG14-1091	V	E-12-03b	1090.5	1085.2	MV	40	59.62 - 60.81	6.66 - 7.37	1.08 - 1.82	24	8455 - 8367	U-3, Ulleungdo	500 NW	-
SG14-1185	C	F-12 (62.0 - 63.0 cm)	1184.0 - 1185.0	1180.2 - 1181.2	MV, MI	40 - 50	67.55 - 77.92	3.03 - 4.38	0.67 - 4.13	18	9372 - 9301	-	-	-
SG06-1288 ³	V	G-03-02	1301.3	1287.9	MV	60	60.49 - 62.00	6.57 - 7.48	1.42 - 2.03	12	10230 - 10171	U-4, Ulleungdo ³	500 NW	6

References 1) McLean et al. (2016); 2) Smith et al. (2013); 3) Smith et al. (2011b); 4) Oppenheimer et al., (2017)

V / C = Visible / Cryptotephra layer

PU = Pumiceous, PL = Platy, C = Cusate, F = Fluted, V = Vesicular, MV = Microvesicular, MI = Microlite Inclusions (see Figure 2)

n = number of analyses

* Sampling range for cryptotephra layers and base of visible ash layers

** General shard length in the fraction extracted, i.e. in the population >25 µm

*** Tephras marked with a dash have not been able to be robustly correlated to a particular tephra or volcano.

4.3. Zone 3

Zone 3 covers the Early Holocene sedimentation at Lake Suigetsu, spanning from the visible (~2 cm thick) U-Oki tephra (SG06-1288; 13.0 m SG14-CD) to the visible (~3 cm thick) K-Ah tephra (SG06-0967; 9.7 m SG14-CD) (Figure 4). The age-model for the Lake Suigetsu sediments constrains the age of these tephra layers and sediments between ~ 10.2 and 7.3 cal. yrs BP. Within Zone 3, two visible and two cryptotephra primary ash layers are identified and labelled by their SG06/SG14-CD: SG06-1288 (visible layer that was correlated to the U-Oki tephra by Smith *et al.*, 2011b), SG14-1185, SG14-1091 (visible) and SG14-1058. These are dated to 10230 – 10171 cal. yrs BP, 9372 – 9301 cal. yrs BP, 8455 – 8367 cal. yrs BP, and 8166 – 8099 cal. yrs BP (95.4% confidence interval), respectively (Table 1).

Glass shards in SG06-1288 (U-Oki tephra) are generally ~ 60 µm in length and are clear to medium brown in colour (Figure 5). The U-Oki shards have a characteristic pumiceous, microvesicular morphology, which are seen in high concentrations for ~2 m (~ 2 ka) after the primary deposition of the visible layer.

SG14-1058 is positioned above a known event layer (Yamada *et al.*, submitted), but is deemed a primary tephra isochron since all observed shards possessed a consistent morphology (highly cusped, with very large elongated vesicles), size and a homogeneous geochemical composition which is distinct from the underlying visible tephra layers. Furthermore, these shard characteristics were not observed in the subsequent 2 meters of older sediments.

Within Zone 3, platy shards were observed between ~10.0 - 10.5 m SG14-CD, and some clear cusped glasses were also observed between ~11 – 13 m SG14-CD. However, there are no clear peaks in these glass concentrations, suggesting either: i) the primary input is obscured within the background glass concentrations, or ii) the isochron is positioned below the U-Oki tephra layer.

4.4. Zone 2

Zone 2 contains the highest concentrations of background glasses, and extends from the visible K-Ah tephra (SG06-0967) at 9.7 m to 3.7 m SG14-CD; ~ 7.3 to 2.2 ka yrs BP (Figure 4). Within Zone 2, three visible and six cryptotephra layers are recognised: visible layer SG06-0967 (previously correlated to the K-Ah tephra by Smith *et al.*, 2013), SG14-0840, SG14-0803, visible layer SG14-0781, SG14-0704, visible layer SG06-0588 (previously characterised by Smith *et al.*, 2013), SG14-0513, SG14-0490 and SG14-0433. These are dated to 7307 – 7196 cal. yrs BP, 5986 – 5899 cal. yrs BP, 5681 – 5619 cal. yrs BP, 4894 – 4827 cal. yrs BP, 4066 – 3986 cal. yrs BP, 3428 – 3312 cal. yrs BP, 3227 – 3129 cal. yrs BP, and 2737 – 2620 cal. yrs BP (95.4 % confidence interval), respectively (Table 1).

Glass shards in SG06-0967 (K-Ah tephra) range in size from 50 – 100 µm, and are clear or brown (minor population) with platy morphologies (Figure 5). These shards are seen in high concentrations (> 5000 shards/gram) for ~1 m of sedimentation following the deposition of the K-Ah visible layer. Since these background glasses are very distinctive, other primary tephra layers with distinctive shard morphologies, such as SG14-0840 (highly cusped and fluted in shape), were easily identified (Figure 5).

4.5. Zone 1

Late Holocene sedimentation in Zone 1 extends from ~3.7 m SG14-CD (2.2 ka) to the core top (Figure 4), and considerably lower background glasses were observed than in Zone 2. One visible and six cryptotephra layers are found within Zone 1. The visible layer is the previously identified B-Tm tephra associated with the 'Millennium' eruption from Changbaishan volcano in China/North Korea (SG06-0226; McLean *et al.*, 2016). Newly identified cryptotephra layers, labelled using their SG14 composite depths, are: SG14-0373, SG14-0317, SG14-0239, SG14-0221, SG14-0058 and SG14-0024, and are dated to 2192 – 2117

cal. yrs BP, 1815 – 1735 cal. yrs BP, 1183 – 1111 cal. yrs BP, 990 – 959 cal. yrs BP, 204 – 48 cal. yrs BP, 30 – -13 cal. yrs BP (95.4 % confidence interval), respectively (Table 1).

The lower levels of background glasses observed during this period are probably because the majority of the K-Ah tephra has worked its way through the catchment. Since there are lower concentrations of background glasses, small peaks (< 2000 shards/gram) in shard concentrations could be more easily identified. Several further peaks in shard concentrations had shards with variable sizes, morphologies and heterogeneous glass compositions (spanning both typical Kikai and Aira glass chemistries). These peaks (labelled B and C on Figure 4) are not deemed primary tephra layers and likely represent flood or secondary reworking events.

5. Glass geochemistry results

Major element glass compositions of the SG14 Holocene tephra layers are presented in Table 2 and selected bi-plots in Figure 6. SG14-0513, SG14-0373, SG14-0317 and SG14-0058 glass shards could not be analysed as they were too small or had too many microlite inclusions (Figure 5). Geochemical analyses of background shards were excluded from the presented datasets but are included in the Supplementary Material.

The most abundant oxides, SiO₂, K₂O, CaO, Al₂O₃ and FeO^T (all Fe as FeO) are predominantly used to characterise and discriminate the tephra layers since they can be precisely measured by the electron microprobe. The glass compositions of the Holocene tephra layers in the Lake Suigetsu record range from phono-trachytic to rhyolitic, with the exception of the dacitic SG14-1185 and SG14-0024 tephra layers (Figure 6). As illustrated in the major element bi-plots and Figure 6e, the glass compositions of the tephra layers are generally homogenous with narrow compositional ranges, with the exception of those from SG14-1185, SG14-0781 and SG06-0588. Some of these tephras have very similar or indistinguishable major element glass compositions, for example, SG06-1288, SG14-1091 and SG14-0803.

Table 2. Glass compositions (normalised) of the SG14 Holocene tephra layers identified in this study (FeO^T = all Fe reported as FeO). Raw dataset and secondary standards are included in the Supplementary Material.

	SG14-0024		SG14-0221		SG14-0239		SG14-0433		SG14-0490		SG14-0704	
wt. (%)	Avg.	± 1 σ	Avg.	± 1 σ	Avg.	± 1 σ	Avg.	± 1 σ	Avg.	± 1 σ	Avg.	± 1 σ
SiO ₂	69.33	0.52	73.43	0.44	77.87	0.21	61.76	0.16	77.14	0.23	72.19	0.75
TiO ₂	0.81	0.03	0.63	0.04	0.08	0.03	0.79	0.05	0.25	0.04	0.56	0.04
Al ₂ O ₃	14.32	0.25	13.15	0.44	12.76	0.16	16.66	0.05	12.57	0.10	13.78	0.66
FeO ^T	4.15	0.21	3.12	0.12	0.54	0.10	5.65	0.17	1.20	0.11	3.18	0.45
MnO	0.13	0.03	0.17	0.04	0.07	0.04	0.23	0.05	0.05	0.04	0.10	0.06
MgO	0.97	0.13	0.77	0.05	0.06	0.04	1.09	0.06	0.29	0.04	0.58	0.13
CaO	3.35	0.20	3.24	0.13	0.39	0.14	2.57	0.08	1.61	0.09	2.63	0.37
Na ₂ O	4.01	0.31	4.47	0.15	4.15	0.23	6.07	0.18	3.92	0.09	3.93	0.16
K ₂ O	2.56	0.06	0.77	0.04	3.90	0.20	4.59	0.10	2.79	0.09	2.82	0.12
P ₂ O ₅	0.23	0.02	0.13	0.04	0.03	0.02	0.36	0.04	0.05	0.02	0.12	0.02
Cl	0.14	0.03	0.14	0.04	0.15	0.04	0.23	0.03	0.12	0.02	0.12	0.02
<i>n</i>	6		14		20		8		19		10	

	SG14-0781		SG14-0803		SG14-0840		SG14-1058		SG14-1091		SG14-1185	
wt. (%)	Avg.	± 1 σ	Avg.	± 1 σ	Avg.	± 1 σ	Avg.	± 1 σ	Avg.	± 1 σ	Avg.	± 1 σ
SiO ₂	76.18	0.95	60.54	0.63	74.15	0.23	75.01	0.18	60.52	0.24	72.29	2.78
TiO ₂	0.16	0.03	0.62	0.07	0.47	0.03	0.20	0.03	0.51	0.08	0.56	0.12
Al ₂ O ₃	13.90	0.57	19.48	0.30	13.50	0.23	10.28	0.11	19.87	0.22	13.75	0.91
FeO ^T	0.90	0.23	3.16	0.42	2.33	0.11	3.89	0.10	2.77	0.24	2.80	0.80
MnO	0.06	0.04	0.14	0.10	0.11	0.05	0.07	0.03	0.15	0.03	0.07	0.04
MgO	0.28	0.14	0.48	0.12	0.61	0.06	0.01	0.01	0.23	0.03	0.63	0.28
CaO	1.87	0.30	1.99	0.33	2.81	0.11	0.20	0.02	1.48	0.14	2.45	0.94
Na ₂ O	3.92	0.30	6.60	0.60	4.57	0.15	5.30	0.16	6.95	0.40	3.46	0.28
K ₂ O	2.55	0.40	6.61	0.21	1.22	0.05	4.50	0.06	7.03	0.19	3.73	3.73
P ₂ O ₅	0.05	0.03	0.17	0.05	0.08	0.02	0.01	0.01	0.05	0.04	0.10	0.04
Cl	0.14	0.05	0.21	0.04	0.11	0.02	0.52	0.02	0.40	0.08	0.12	0.04
<i>n</i>	27		19		25		25		24		18	

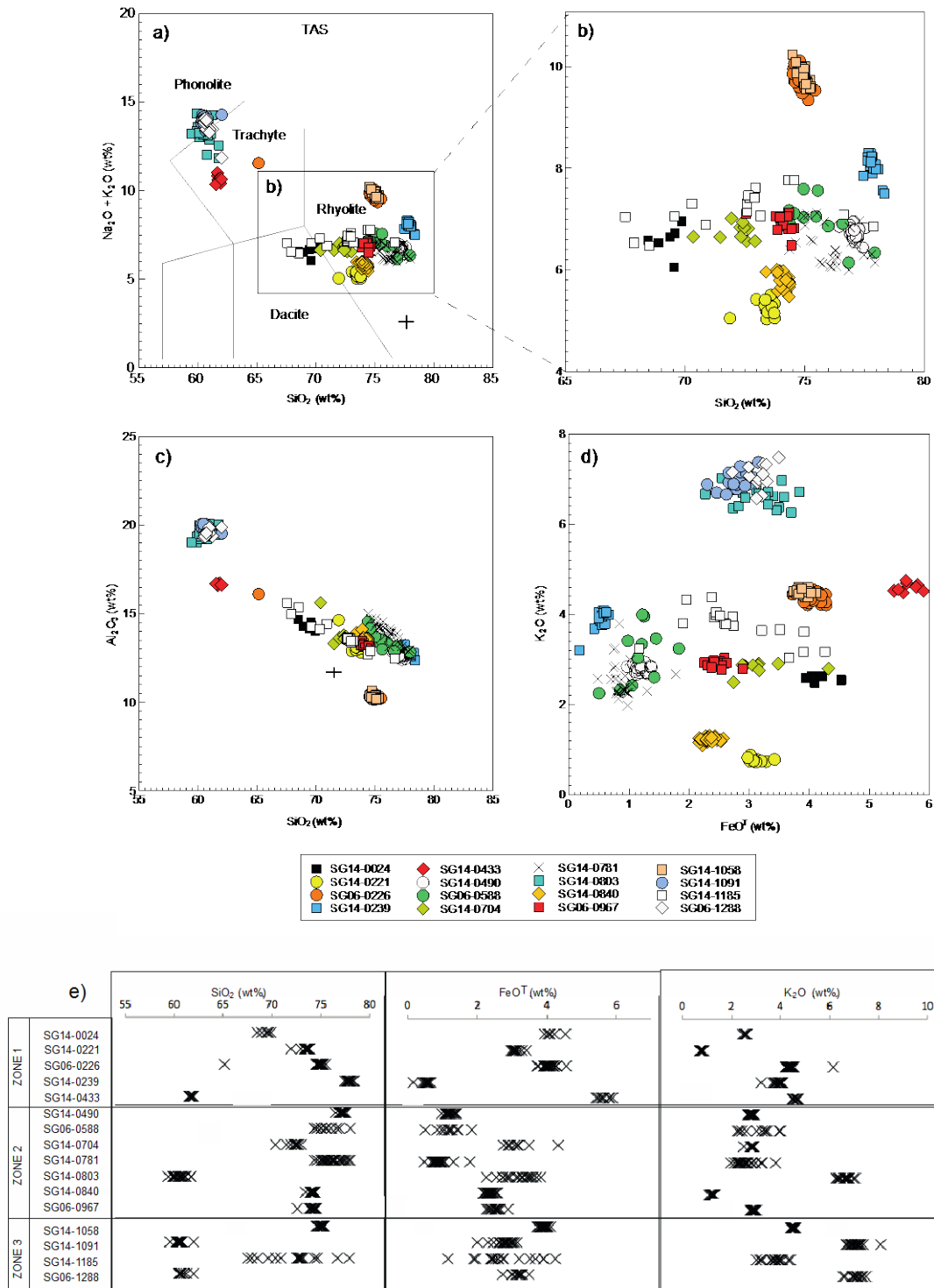


Figure 6. Major element compositions of the tephra layers within the Holocene sediments of the Lake Suigetsu SG14 core. These tephras are labelled using their SG06/SG14 composite depths. (a) Total alkalis versus silica plot (TAS; with whole-rock classifications based on Le Bas *et al.*, 1986), (b, c, d) Bivariate plots for SiO_2 , FeOT , K_2O and Al_2O_3 compositions (error bars represent 2 x standard deviation of repeat analyses of the StHs6/80-G MPI-DING standard glass), (e) SiO_2 , FeOT , K_2O compositions of Holocene tephras that have been analysed from Lake Suigetsu (SG06 and SG14) versus stratigraphic position (including data from Smith *et al.*, 2011b; Smith *et al.*, 2013; McLean *et al.*, 2016).

The glasses range from low-K (tholeiitic) through to high-K (calc-alkaline and shoshonitic) compositions (Figure 7), which can be used to discriminate between the different volcanic regions in East Asia. Back-arc volcanoes in South Korea (Ulleungdo) and North Korea/ China (Changbaishan) erupt K₂O-rich (> 3 wt. %) glasses, which contrast with eruption deposits from Hokkaido and northern Honshu that typically have < 1 wt. % K₂O (Machida and Arai, 2003; Smith *et al.*, 2013). Tephra layers with different ages that possess similar or identical geochemical compositions are likely to represent eruptions from the same or closely located volcano (e.g., Shane, 2000; Smith *et al.*, 2005; Albert *et al.*, 2012; 2017).

The glass morphology, relative stratigraphy, geochemical compositions and precise chronology of the tephra layers, were used to correlate the SG14 Holocene isochrons to their volcanic sources and specific eruptions. The glass compositions of the SG14 tephra layers were compared to new (Supplementary Material) and published compositions obtained from proximal outcrops with known eruption deposits. These compositions indicate that the SG14 tephra layers are from the following volcanoes or regions:

1. North Korea/China: Changbaishan - SG14-1058 and SG06-0226.
2. South Korea: Ulleungdo - SG06-1288, SG14-1091, SG14-0803 and SG14-0433.
3. Northern Japan: Towada - SG14-0840, and Mashu - SG14-0221.
4. Southwest Japan: Kawagodaira - SG14-0490, and Kozushima - SG14-0239.
5. Southern Japan: Kikai - SG06-0967 and SG14-0704.

These correlations and geochemical compositions are discussed below along with the other tephra that have not yet been correlated to known eruptions or volcanoes.

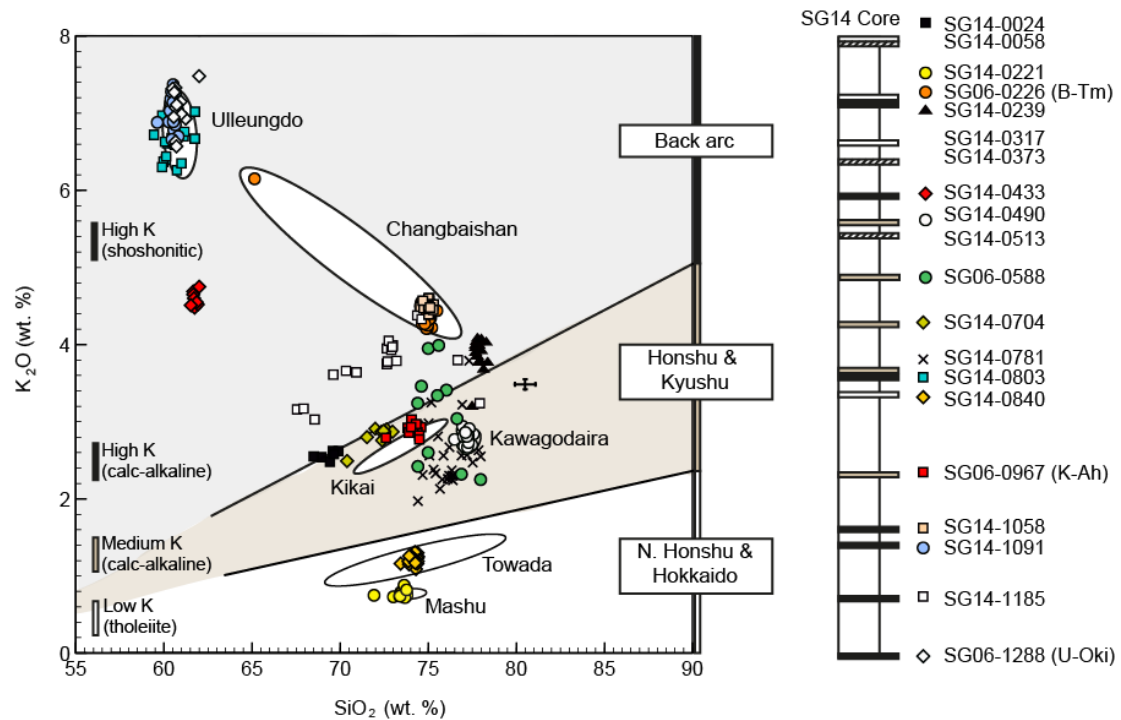


Figure 7: SiO_2 and K_2O glass compositions of the SG14 tephra layers (labelled using their SG14 composite depths) compared to proximal glasses originating from the back-arc volcanism from South Korea (Ulleungdo = U-Ok; Smith *et al.*, 2011b), North Korea/China (Changbaishan = B-Tm; Chen *et al.*, 2016; McLean *et al.*, 2016), and the Japanese arc (Arai = AT, Kikai = K-Ah from Smith *et al.*, 2013; and Kawagodaira = KGP, Towada = To-Cu and Mashu = Ma-b from this study). Glass analyses are plotted on the whole-rock K-classification scheme of Peccerillo and Taylor (1976). The back-arc and intraplate volcanism produces high-K (shoshonitic) compositions, which contrast to the eruptive products from northern Honshu and Hokkaido, which have low-K (tholeiite) compositions. Geochemical analyses of SG14-0058, SG14-0373 and SG14-0513 could not be obtained due to their small shard sizes and/or abundance of microlite inclusions. Error bars represent 2 x standard deviation of repeat analyses of the StHs6/80-G MPI-DING standard glass.

6. Source of the tephra layers

6.1. Changbaishan tephra layers (SG14-1058 and SG06-0226)

Changbaishan (also referred to as Baitoushan, Baekdusan, Paektu and Hakutosan) volcano is situated on the border of North Korea and China (128°03'E, 41°00'N), and almost 1000 km NW of Lake Suigetsu (Figure 1). Despite evidence of numerous highly explosive episodes during the Quaternary (Machida *et al.*, 1990; Lim *et al.*, 2013), and recent seismic activity (Xu

et al., 2012), the eruptive history of Changbaishan volcano has not been established (Wei *et al.*, 2003; Ramos *et al.*, 2016; Pan *et al.*, 2017). This is largely due to the difficulties in accessing the proximal outcrops, and that successive eruption deposits are geochemically indistinguishable (Lim *et al.*, 2013). Several eruption deposits, potentially of Holocene age have been identified proximally, however this stratigraphy and chronology varies considerably across studies (see Pan *et al.*, 2017). Consequently, distal archives are essential to establish the number of eruptions and date past explosive activity from Changbaishan.

The B-Tm tephra (AD 946; Oppenheimer *et al.*, 2017; Hakozaik *et al.*, 2017) is the only confirmed distal layer from Changbaishan Holocene activity. This was dispersed during the highly explosive 'Millennium' eruption, which was one of the most violent in the past 2000 years (see Sun *et al.*, 2014b). The B-Tm tephra has been identified in numerous marine, lacustrine and archaeological sequences across central Japan, northeast China and coastal regions of Russia (see McLean *et al.*, 2016). Furthermore, B-Tm glass shards have also been identified in the Greenland ice cores (Sun *et al.*, 2014a). Tephra layer SG06-0226 has previously been correlated to the B-Tm tephra (McLean *et al.*, 2016) and currently presents the most southerly occurrence of this isochron. The precise age (AD 946; Oppenheimer *et al.*, 2017; Hakozaik *et al.*, 2017) is incorporated within the Lake Suigetsu age model to constrain the chronology of the upper portion of the core.

The Changbaishan compositions can easily be distinguished from the lower alkali glasses produced from the Japanese arc, and the phonolitic glasses from Ulleungdo, South Korea (Figure 7). The SG14 core contains an additional isochron (SG14-1058) that has glass compositions that are consistent with those erupted at Changbaishan (Figure 8). SG14-1058 glass compositions overlap on all major elements with the rhyolitic member of SG06-0226 (B-Tm ash), and glasses from the B-Tm distal type-site (Tomakomai Port; McLean *et al.*, 2016), with SiO₂ ranging from 74.5 – 75.3 wt. %, K₂O from 4.4 – 4.6 wt.% and CaO ~0.2 wt. % (Figure 8b; Figure 8c). This geochemical affinity is consistent with the identical compositions of older eruptions from Changbaishan, observed as thick deposits in the Sea of Japan (Lim *et al.*, 2014). The Lake Suigetsu tephrostratigraphy therefore provides the first evidence for an

additional Holocene eruption from Changbaishan at 8166 – 8099 cal. yrs BP (95.4% confidence interval) (Table 1).

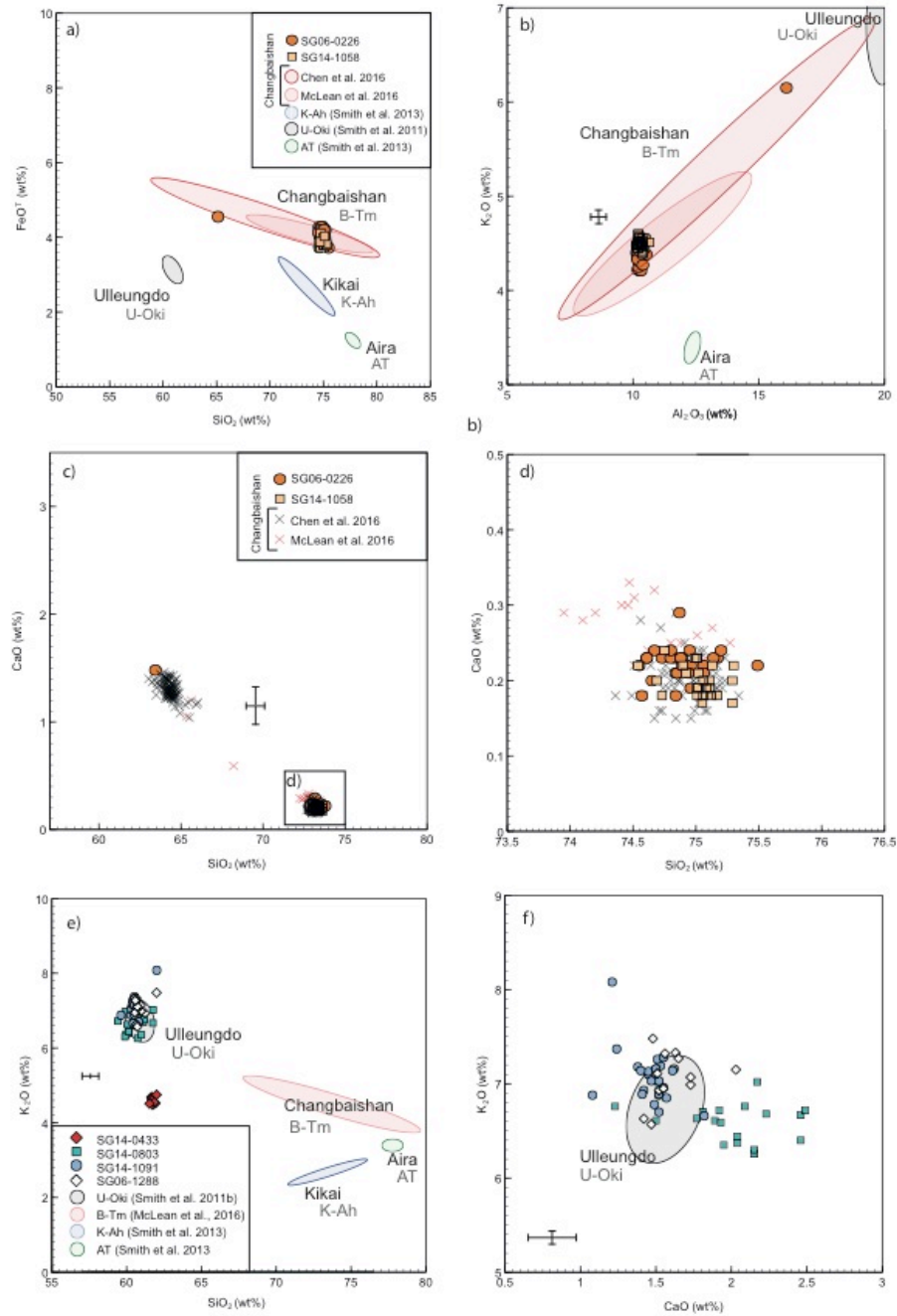


Figure 8: Glass shard major element compositions of: (a, b, c, d) tephra layers SG14-1058 and SG06-0226 compared to Changbaishan (B-Tm) glasses (Chen *et al.*, 2016; McLean *et al.*, 2016), and (e, f) tephra layers SG14-0803, SG14-1091 and SG06-1288 (U-Oki ash) compared to Ulleungdo (U-Oki) glasses (Smith *et al.*, 2011b). Proximal compositional fields are labelled by volcano (black) and tephra (grey). Error bars represent 2 x standard deviation of repeat analyses of the StHs6/80-G MPI-DING standard glass.

6.2. Ulleungdo tephra layers (SG06-1288, SG14-1091, SG14-0803 and SG14-0433)

Ulleungdo volcano is an island located in the southwest Japan Sea (37°30'N 130°52'E), ~110 km from the Korean Peninsula and ~500 km NW of Lake Suigetsu (Figure 1). Ulleungdo is known to have erupted four times during the Holocene, as determined by proximal deposits identified on the island (Machida *et al.*, 1984; Shiihara *et al.*, 2011). These are proximally named (oldest to youngest): U-4, U-3, U-2 and U-1, and the K-Ah tephra positioned between the U-3 and U-2 deposits. The largest known Plinian eruption from Ulleungdo generated the Ulleung-Oki (U-Oki) tephra layer (Machida and Arai, 1983; Okuno *et al.*, 2010; Lim *et al.*, 2014), which equates to the proximal U-4 of Shiihara *et al.*, (2011). The U-4 eruption is dated using the Lake Suigetsu chronology to have occurred between 10230 – 10171 cal. yrs BP (95.4 % confidence interval; Smith *et al.*, 2011b; Staff *et al.*, 2011) (Table 1). The U-3 eruption has been dated (¹⁴C of charcoal preserved within the proximal eruption deposits) to 8440 – 8360 cal. yrs BP (95.4% confidence interval; Im *et al.*, 2012; Kim *et al.*, 2014) and the U-2 has been dated to 5749 – 5604 cal. yrs BP (Okuno *et al.*, 2010). The youngest U-1 eruption is considered to be from a small strombolian eruption and has not been dated (Kim *et al.*, 2014).

The U-Oki (U-4) tephra is a key widespread marker bed found in most sedimentary sequences east of Ulleungdo, in the Sea of Japan and central Honshu (Figure 1). Distal equivalents of the U-3 eruption have also been reported in the Sea of Japan (TRG1 sediment core; Domitsu *et al.*, 2002), Lake Biwa (Nagahashi *et al.*, 2004) and close to Hakusan volcano, central Honshu (Higashino *et al.*, 2005). U-2 and U-1 have only been found on the flanks of the volcano (Kim *et al.*, 2014).

Glass compositions from Ulleungdo are distinctively alkali-rich, containing ~ 6.5 wt. % higher K₂O, and ~ 15 wt. % lower SiO₂ (~60 wt. %) compared to eruptive products from the Japanese arc (Smith *et al.*, 2011b; Smith *et al.*, 2013). Ulleungdo glasses are also typically higher in K₂O content than the trachytic (lower SiO₂) end-member of Changbaishan eruptive products (Figure 7). Proximal compositions from the Holocene eruptions of Ulleungdo (U-4,

U-3 and U-2) straddle the phonolite-trachyte boundary and appear to be indistinguishable on major and trace element compositions (Shiuhara *et al.*, 2011). No glass compositions have been published for the U-1 eruption.

Three tephra layers in the Lake Suigetsu cores (SG06-1288, SG14-1091 and SG14-0803) contain alkali-rich glasses from Ulleungdo (Figure 8e, Figure 8f; Smith *et al.*, 2011b), and represent the distal equivalents of proximal deposits of U-4, U-3 and U-2, respectively. The geochemical compositions obtained from the U-4 (SG06-1288) and U-3 (SG14-1091) glasses preserved in Lake Suigetsu are indistinguishable using major and minor element compositions. However, we find the younger SG14-0803/U-2 glasses are more elevated in CaO (by ~0.5 wt. %) compared to the early Holocene eruptions, SG06-1288/U-4 and SG14-1091/U-3 (Figure 8f). Furthermore, SG14-0803/U2 glass shards contain a greater portion of brown, highly vesicular, pumiceous shards (Figure 5), which may also help to distinguish this layer from the older Ulleungdo deposits elsewhere. The modelled ages of SG14-1091 (8455 – 8367 cal. yrs BP) and SG14-0803 (5681 – 5619 cal. yrs BP) (95.4% confidence interval) are in agreement with the published chronological information and further constrain the dates for U-3 and U-2.

SG14-0433 glass compositions also contain ~ 60 wt. % SiO₂, but have ~ 2.5 wt. % lower K₂O, and ~2 wt. % higher CaO compared to the typical compositions erupted during large explosive eruptions from Ulleungdo (Figure 8e; Table 2). Since no other volcanoes in this region, especially those along the Japanese arc, produce such evolved compositions; it suggests that SG14-0433 is a distal occurrence of U-1. The age of this tephra (2737 – 2620 cal. BP) is consistent with a repose interval of < 3 ka throughout the Holocene.

6.3. Towada (SG14-0840) and Mashu (SG14-0221) tephra layers

Towada is a large caldera, situated in northern Honshu (40°28'N 140°52'E), ~700 km NE of Lake Suigetsu (Figure 1). Towada has erupted repeatedly throughout the Holocene, the largest of which dispersed the Towada-Chuseri (To-Cu) ash across northern Honshu and the

coastal regions of the Pacific (Machida and Arai, 2003; Figure 1). In proximal localities, three eruptive units are recognised in the To-Cu sequence, an opening Plinian fall (named Chuseri), which is overlain by the Kanagasawa pumice fall and topped by the Utarube ash, a dilute pyroclastic density current (PDC), deposit (Hayakawa, 1985). All three units of To-Cu are predominantly recorded to the east of the volcano (Hayakawa, 1985; Figure 1).

The To-Cu eruption is proximally dated to 6293 – 6029 cal. yrs BP based upon a ^{14}C age of charcoal fragments preserved in the dilute PDC deposits (Hayakawa, 1983). Furthermore, the soil beneath the To-Cu is dated to 6313 – 6180 cal. yrs BP (Inoue *et al.*, 2011), providing a maximum age constraint for the eruption. As observed for other volcanoes situated in northern Honshu and Hokkaido, the tholeiitic glasses from Towada contain low K_2O (< 1.5 wt. %) and between 5 – 6 wt. % total alkalis (Figure 9). Glass analyses of the three proximal units from To-Cu (Supplementary Material) show that the Plinian Chuseri pumice fall deposits are more homogenous than the overlying Kanegasawa and Utarube eruptive units (Figure 9d; Supplementary material).

The SG14-0840 glasses are geochemically indistinguishable from the proximal compositions of the To-Cu ash (Figure 9); in particular the glass compositions at Lake Suigetsu sit within the tight geochemical range of the Chuseri Plinian pumice fall (Figure 9d). This suggests that only ash from the initial Plinian phase of the eruption reached Lake Suigetsu/central Honshu. The Lake Suigetsu age model provides an eruption age of To-Cu of 5986 – 5899 cal. yrs BP (95.4% confidence interval; Table 1), which is marginally younger than proposed by Hayakawa (1983).

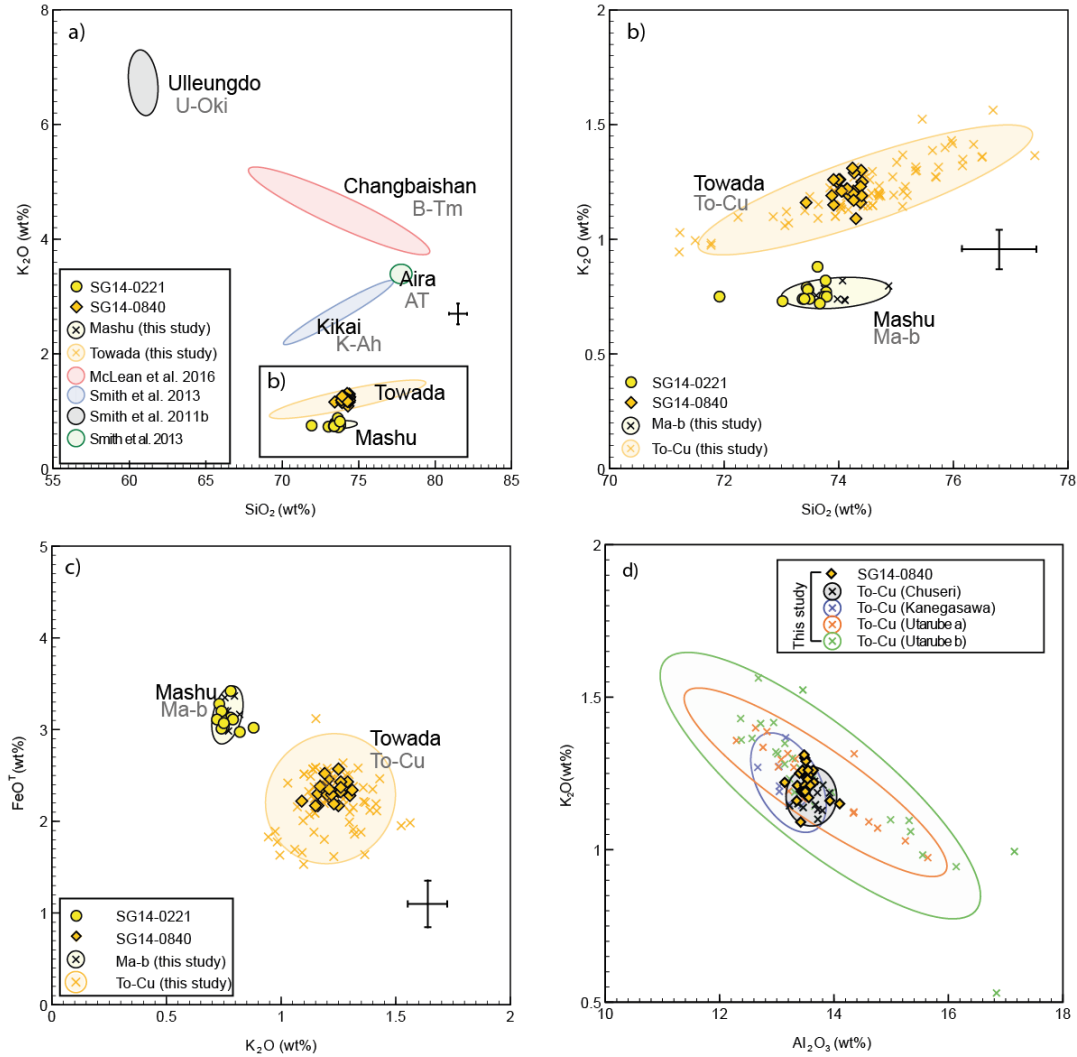


Figure 9: Glass shard major element compositions of tephra layers SG14-0221 and SG14-0840 compared to proximal glass compositions from Towada (To-Cu, this study) and Mashu volcano (Ma-b, this study). Glass compositions for other large explosive eruptions from Ulleungdo (U-Oki; Smith *et al.*, 2011b), Kikai (K-Ah, Smith *et al.*, 2013), Aira (AT, Smith *et al.*, 2013) and Changbaishan (McLean *et al.*, 2013) volcanoes are also shown for comparison. Glasses from northern Honshu and Hokkaido have low-K compositions (tholeiite). Volcano (black) and tephra (grey) labels indicate the glasses used to generate the compositional fields. Error bars represent 2 x standard deviation of repeat analyses of the StHs6/80-G MPI-DING standard glass.

Mashu volcano (43°35'N 144°31'E) is situated on the eastern side of Kutcharo caldera in eastern Hokkaido (Figure 1) and is 1160 km NE of Lake Suigetsu. The most recent phase of activity (during the cone building) at Mashu volcano produced three widespread distal ash

layers: Ma-c2, Ma-c1 and Ma-b, the youngest (Ma-b) was a large eruption with a Volcanic Explosivity Index (VEI; Newhall and Self, 1982) of 5, which ejected 4.6 km³ DRE (dense rock equivalent) of magma (Kishimoto *et al.*, 2009). This Ma-b eruption dispersed ash directly southwards (Machida and Arai, 2003), and forms an isochronous marker in several palaeoenvironmental and archaeological sequences in eastern Hokkaido (Wada *et al.*, 2001; Nakagawa *et al.*, 2002; Nakamura *et al.*, 2009). The Ma-b eruption is dated to have occurred between 976 and 774 cal. yrs BP (AD 974 – 1176; Shoji and Masui, 1974).

Glasses erupted during the Holocene activity of Mashu are very low in K₂O (< 1 wt. %) (Nakamura, 2016) and ~ 0.5 wt. % lower than glass compositions from Towada volcano (Figure 9; Supplementary Material). The proximal deposits of the Ma-b eruption have homogenous glass compositions (~73 wt. % SiO₂, ~13 wt. % Al₂O₃ and ~ 3 wt. % CaO; Supplementary Material). Geochemically, the tholeiitic glasses of SG14-0221 are indistinguishable from those of the Ma-b tephra, confirming Mashu (Ma-b) is the source of this ash fall event in Lake Suigetsu. The Lake Suigetsu age model provides the most precise age for the Ma-b eruption (due to the chronological constraint imposed on this portion of the Lake Suigetsu record by the B-Tm ash, dated to AD 946; Oppenheimer, 2017; Hakozaik *et al.*, 2017), of 990 – 958 cal. yrs BP (AD 960 – 992; 95.4% confidence interval).

6.4. Kawagodaira (SG14-0490) and Kozushima (SG14-0239) tephra layers

Kawagodaira (34°51'N 138°58'E) is situated on the northwest slope of Amagi volcano, and forms part of the Izu-Tobu cluster of cones on the Izu Peninsula, 290 km E of Lake Suigetsu (Figure 1). The Kawagodaira pumice (KGP) was dispersed during a mid-Holocene eruption from this volcano, and forms a marker layer in sedimentary archives across the central and western parts of Honshu (Hamuro, 1977; Ikeya *et al.*, 1990; Shimada, 2000; Takemura *et al.*, 2010; Figure 1). The KGP tephra layer is very precisely dated by radiocarbon wiggle-matching of a Japanese cedar timber, which was found charred within pyroclastic density deposits of the eruption (Tani *et al.*, 2013), to 3151 – 3126 cal. yrs BP (95.4% confidence interval).

Glasses preserved in proximal deposits of the KGP ash span a broad compositional range, with SiO₂ from 77.1 to 77.8 wt. %, CaO from 1.5 to 1.6 wt. %, and K₂O from 2.6 to 2.8 wt. % (Figure 10a; Figure 10b; Supplementary Material). The SG14-0490 glasses share the same composition, providing a confident correlation to the KGP. The existing Lake Suigetsu age model provides an age of 3227 – 3129 cal. yrs BP (95.4% confidence interval) for the distal KGP tephra (SG14-0490), which overlaps with the wiggle-matched age of the cedar wood from the PDC deposits (Tani *et al.*, 2013). This wiggle-matched age is very precise and therefore, was incorporated into the updated Lake Suigetsu age model presented herein to further constrain the chronology of this portion of the core stratigraphy.

Kozushima (34°12'N 139°09'E), a volcanic island on the Izu arc, 340 km E of Lake Suigetsu (Figure 1), has erupted 18 rhyolitic lava domes that have also been accompanied by explosive phases. The youngest dome, Tenjo-san, was last active during AD 838, which dispersed the distal ash Izu-Kōzushima-Tenjosan (Iz-Kt) tephra westwards (Machida and Arai, 2003). The age of this eruption is recorded in several historical documents including the *Shoku Nihon Koki*, an officially commissioned Japanese historical text (Tsukui *et al.*, 2006). Distally, the Iz-Kt is difficult to stratigraphically and geochemically distinguish from the Nijima-Mukai-yama (Iz-Nm) tephra (Sugiuchi and Fukuoka, 2005; Kobayashi *et al.*, 2007; Suzuki *et al.*, 2017; Tsuchiya *et al.*, 2017), which was dispersed during an eruption from Nijima volcanic island (20 km north of Kozushima) and believed to have occurred in AD 886 (Tsukui *et al.*, 2006).

SG14-0239 glasses overlap the average glass compositions known for both Iz-Kt and Iz-Nm ash layers (Figure 10a; Figure 10b; Suzuki *et al.*, 2017; Sugiuchi and Fukuoka, 2005). The existing Lake Suigetsu age model provides an age of AD 839 – 767 (95.4 % confidence interval) for the SG14-0239 tephra, which overlaps with the Iz-Kt historical age, and suggests SG14-0239 is too young to correlate to the Iz-Nm tephra. This precise historical age of AD 838 is now incorporated into the Lake Suigetsu age model herein at the position of the SG14-0239/Iz-Kt tephra to further constrain the chronology of this portion of the core.

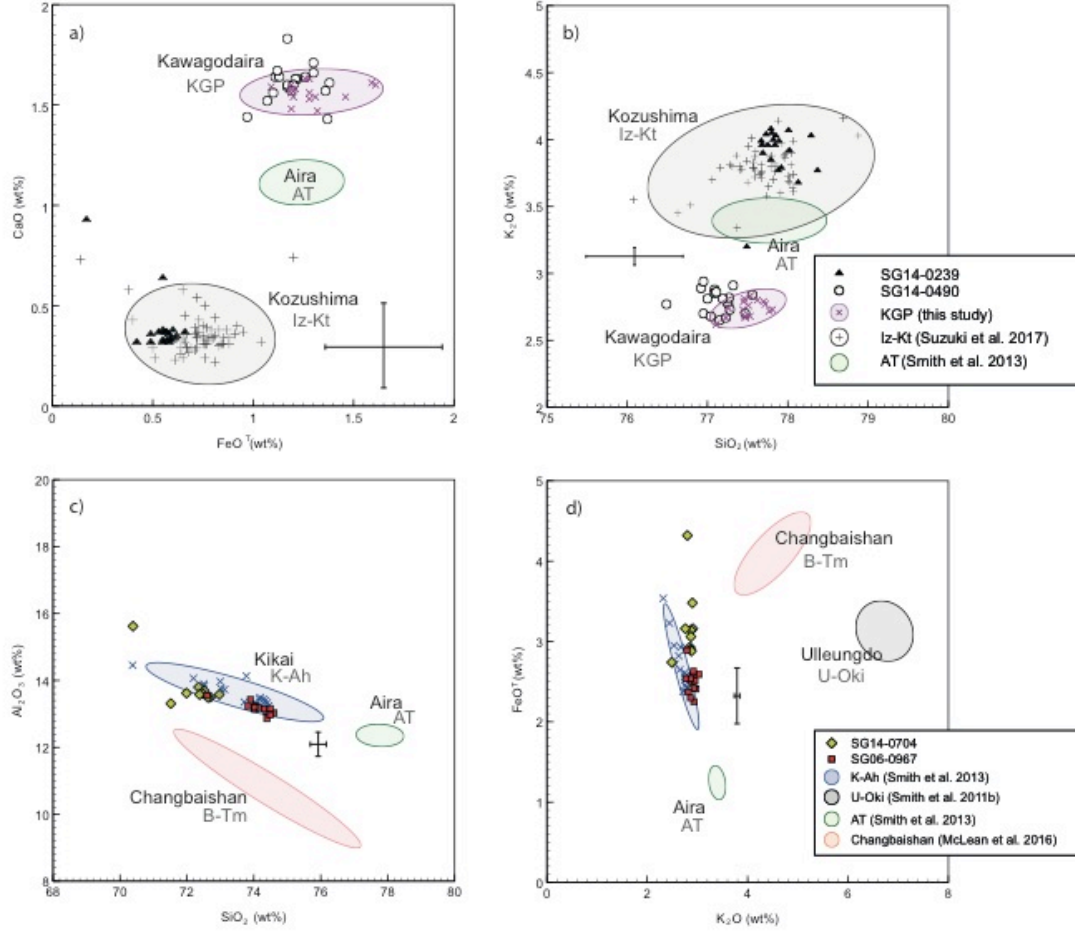


Figure 10. Glass shard major element compositions of: (a, b) tephra layers SG14-0239 and SG14-0490 compared to proximal glass compositions from Kawagodaira (KGP; this study) and Kozushima (Iz-Kt; Suzuki *et al.*, 2017) volcanoes, and (c, d) tephra layers SG14-0704 and SG06-0967 (K-Ah ash) compared to other large explosive eruptions from Ulleungdo (U-Oki; Smith *et al.*, 2011b), Aira (AT; Smith *et al.*, 2013) and Changbaishan (B-Tm; McLean *et al.*, 2013). Error bars represent 2 x standard deviation of repeat analyses of the StHs6/80-G MPI-DING standard glass.

6.5. Kikai tephra layers (SG06-0967 and SG14-0704)

Kikai caldera (30°47'N 130°18'E) is an active volcano situated 50 km south of Kyushu (Figure 1) and was responsible for the most recent VEI 7 Japanese eruption, which dispersed the Kikai-Akahoya (K-Ah) ash over much of Japan, the Sea of Japan, the Pacific Ocean and the East China Sea (Machida and Arai, 1983). This was one of the largest eruptions during the Holocene, alongside the Changbaishan 'Millennium', Mazama (Crater Lake; Bacon and

Lanphere, 2006) and Minoan eruptions (Santorini; Watkins *et al.*, 1978) eruptions. The SG06-0967 layer at Lake Suigetsu is correlated to the K-Ah ash (Figure 10c; Figure 10d; Smith *et al.*, 2013) and was deposited between 7307 – 7196 cal. yrs BP (95.4 % confidence interval).

The Lake Suigetsu K-Ah glass compositions are geochemically homogenous, with SiO₂ ranging from 72.6 – 74.6 wt. %, K₂O from 2.8 – 3.0 wt. % and CaO from 1.8 – 2.3 wt. % (Figure 10c; Figure 10d; Smith *et al.*, 2013). However, glass chemistries obtained by Smith *et al.*, (2013) from medial ash deposits suggests that the K-Ah eruption was more heterogeneous, with SiO₂ ranging from 70.4 – 77.8 wt. %. Interestingly, the younger SG14-0704 glass compositions overlap with the less evolved end-member of the K-Ah medial tephra (Smith *et al.*, 2013; Figure 10c), which suggests that the SG14-0704 tephra could correlate to another eruption from Kikai caldera. SG14-0704 is dated to 4894 – 4827 cal. yrs BP (95.4 % confidence interval) via the Lake Suigetsu chronology, which does not correlate to any known eruption events from Kikai (Moriwaki *et al.*, 2016). Many of the Holocene eruptions from in and around Kyushu Island are poorly dated and lack detailed geochemical data, which means it is problematic to robustly correlate these events. Additional geochemical datasets are required from proximal deposits in the south of Japan to strengthen this potential correlation.

6.6. Tephra layers pending further analysis for correlation

The rhyolitic glasses from visible tephra layers SG14-0781 (5519 – 5480 cal. yrs BP) and SG06-0588 (4066 – 3986 cal. yrs BP) are compositionally heterogeneous, spanning broad SiO₂, FeO_t, CaO and Al₂O₃ ranges that are typical of central Japan arc volcanism (Table 1; Figure 7). Visible tephra layers with similar compositions are also observed in the older SG06 sediments (Smith *et al.*, 2013), suggesting that they are older eruptions from the same volcanic source/s or region. Both SG14-0781 and SG06-0588 contain shards with similar morphologies (i.e. pumiceous and densely vesicular), which are also observed in SG14-0513, SG14-0373 and SG14-0058 cryptotephra layers. Chronologically, SG14-0781 and SG06-0588 are consistent with ages of known Holocene eruptions at Sambe volcano (Figure 1), the

Shigaku S2 and Taiheisan tephra layers (Fukuoka and Matsui, 2002), but there are no proximal datasets for these units. The geochemical assessments of these layers and other pre-Holocene activity at Sambe are further explored by Albert *et al.*, (submitted).

SG14-1185 glass compositions are not consistent with those known from Japan or from Changbaishan or Ulleungdo (Figure 7), and therefore may originate from a more distal volcanic source. The compositional range is similar to glasses from Kamchatka (Ponomareva *et al.*, 2017), however slight differences in FeO^{T} , Na_2O and CaO place SG14-1185 on a different evolutionary trend and preclude a correlation at this time. The source of this tephra layer is currently unknown, and it could represent a very far-travelled ash layer.

7. Discussion

7.1 An integrated tephrostratigraphic framework

The Lake Suigetsu record provides the most comprehensive Holocene tephrostratigraphy for the East Asian/Pacific region, with twenty isochrons from at least nine different volcanic centres (Figure 11). This new framework precisely dates and integrates ash layers from across Japan, South Korea (Ulleungdo volcano) and North Korea/China (Changbaishan volcano), and therefore is a key tephrostratotype for correlating and dating records in this region (Figure 12). These results clearly demonstrate the potential of cryptotephra analysis, even in a productive arc setting, to identify new isochrons from distal sources and provide new insights into the dispersal characteristics and age of these eruptions.

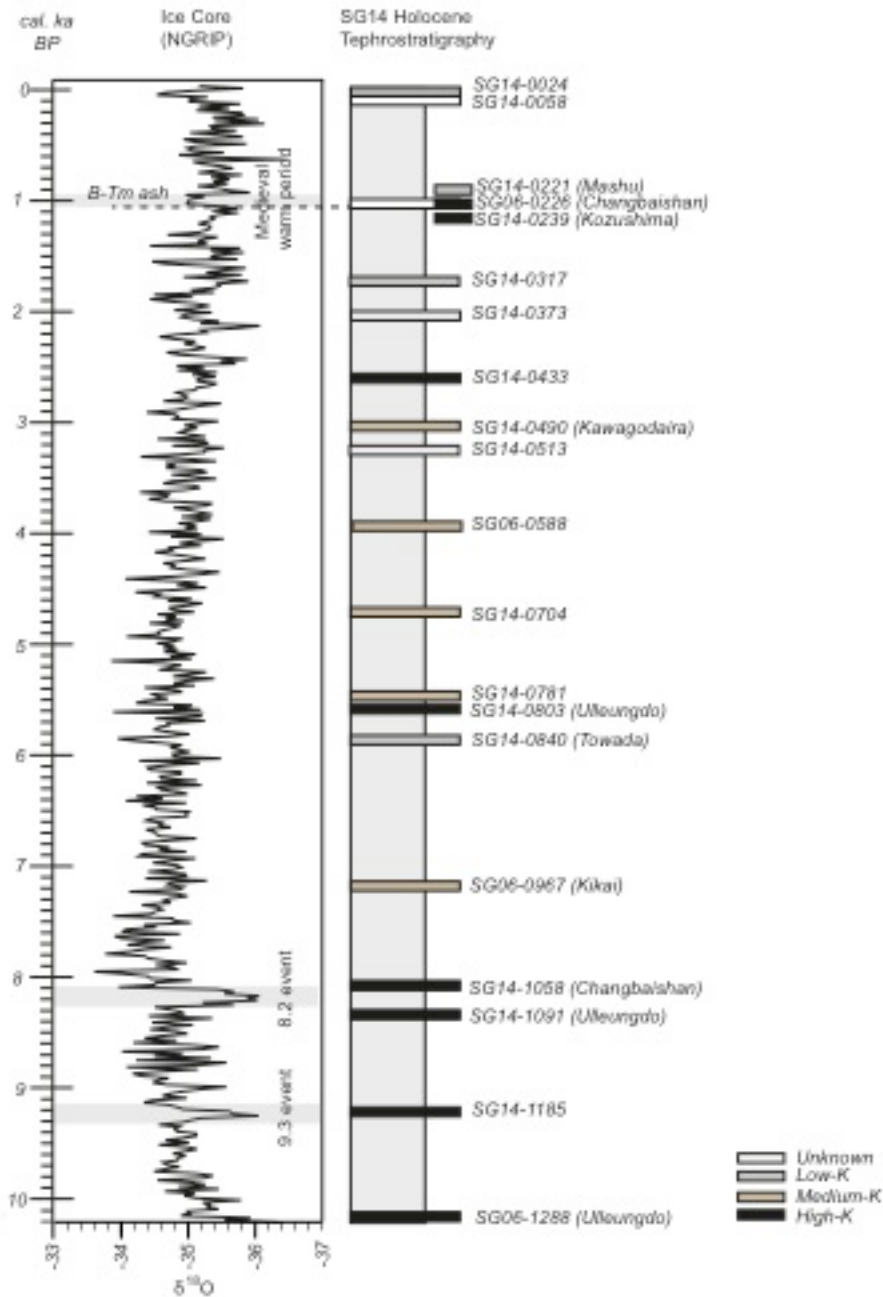


Figure 11. Summary of the Lake Suigetsu Holocene tephrostratigraphy, and the positioning of isochrons against the Greenland ice core (NGRIP) $\delta^{18}\text{O}$ record. The B-Tm ash (AD 946; Oppenheimer *et al.*, 2017) is identified in both high-resolution archives, and occurs close to the onset of the Medieval Warm Period climate anomaly. The K-content of the glasses in these isochrons (see Figure 7) is shown. A few distinctive tephra are recorded in Lake Suigetsu during the early Holocene, which occur close to several rapid climatic anomalies, such as the 8.2 ka event that is observed in Greenland. These marker layers could be used to establish whether these events are synchronous with anomalies recorded in Japan.

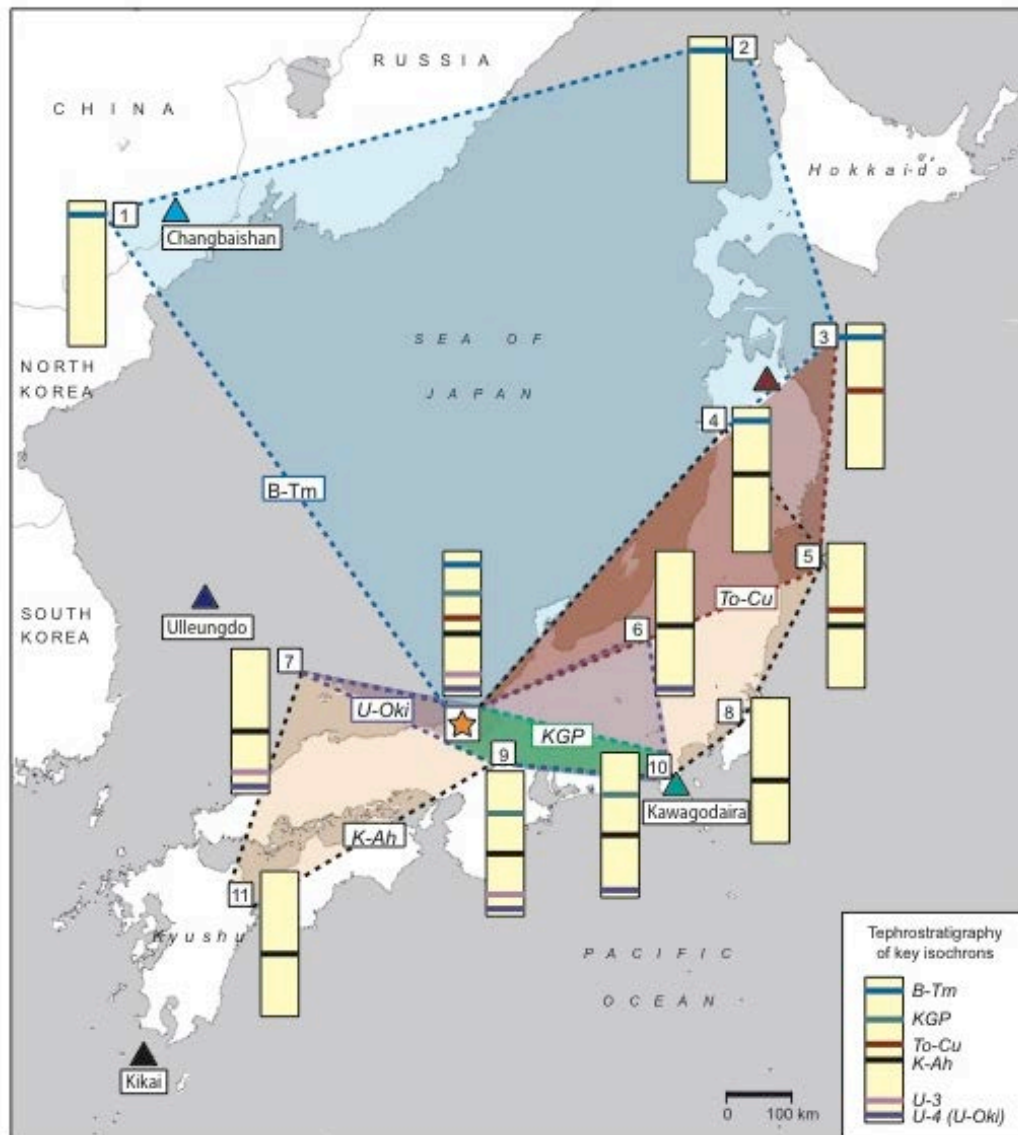


Figure 12. Holocene sections of sedimentary archives (numbered squares) situated in eastern China and Japan that can be integrated using the widespread B-Tm, KGP, To-Cu, K-Ah, U-3 and U-4 (U-Oki) tephra layers. [1] Longgang volcanic field (Sun *et al.*, 2015); [2] Lake Kushu (Chen *et al.*, 2016); [3] Sanriku Coast (Ishimura *et al.*, 2014); [4] Lake Ichi-no-Megata, (Okuno *et al.*, 2011); [5] SK-2 core (Sagawa *et al.*, 2014); [6] Lake Nojiri (Kumon *et al.*, 2003); [7] KT96-17 P-2 (Domitsu *et al.*, 2002); [8] Lake Aoki (Adhikari *et al.*, 2002); [9] Lake Biwa (Nagahashi *et al.*, 2004); [10] Ukishima-ka-hara (Fujiwara *et al.*, 2007); [11] Beppu Bay (Yamada *et al.*, 2017). Tephra layers identified in the Lake Suigetsu sequence originate from several different volcanic sources in the East Asian/Pacific region and thus can be used to precisely integrate terrestrial and marine records spanning these dispersal axes.

The cryptotephra study from Lake Suigetsu has significantly extended the known ash dispersal of numerous key Holocene marker layers, including the Ma-b, Iz-Kt, To-Cu, U-2 and U-3 tephra layers, and has also identified tephra from eruptions with primary plume dispersals in the opposite direction (e.g., To-Cu; Figure 1). Previously, the Ma-b ash had only been found in SE Hokkaido, but is now confirmed over 1100 km from its source as a cryptotephra marker in the Lake Suigetsu SG14 core. This establishes the Ma-b tephra as one of the most widely dispersed Japanese Holocene isochrons, and suggests that it may be preserved in more terrestrial and marine sedimentary sequences across East Asia.

In this study, we have discovered several new previously unreported ash layers, which have now been incorporated within the master tephrostratigraphic framework for this region. One previously unknown eruption from Changbaishan is now confirmed (dated to 8166 – 8099 cal. yrs BP; 95.4% confidence interval), which provides significant development in resolving the poorly constrained explosive history of this volcano. These previously unreported distal ash layers are either from eruptions that are not preserved in the proximal eruption sequences, or the reported ages from the proximal deposits are incorrect.

7.2. Resolving the tempo of East Asian volcanism

The exceptional chronology of the Lake Suigetsu sediments enables us to provide precise and constrained eruption ages for the tephra layers (Table 1). This chronology has significantly improved the eruption ages for many significant explosive events, like the large (VEI 5) Holocene eruption of Mashu (Ma-b tephra), which now has a reduced uncertainty of ~170 years (95.4% confidence interval). The improved eruption ages for many of these key widespread ash layers can now be incorporated into other site-specific age models containing these markers, meaning it may be of significant benefit to specifically search for such isochrons in these records. Furthermore, since many of these marker layers were dispersed across the Pacific and/or the Sea of Japan, like those originating from Ulleungdo, our terrestrially-based ages can be used to circumvent reservoir offsets that result in inaccurate radiocarbon-based marine chronologies (e.g., Ikehara *et al.*, 2011).

The detailed Lake Suigetsu tephrostratigraphy has significant importance for hazard assessment studies in the East Asian/Pacific region. For example, Suigetsu is the first distal record to unequivocally contain, characterise and date three successive Holocene eruptions from Ulleungdo (U-4, U-3, and U-2 tephra layers) and most likely contains the first distal evidence of the U-1 event. The uncertainty of the U-2 eruption has now been significantly reduced (by ~ 25 years), which indicates that there was a repose interval of ~ 2.8 ka following the U-3 eruption. If SG14-0433 is confirmed as a tephra isochron of the U-1 eruption, a very similar repose interval of ~ 3.0 ka is also calculated. It is likely that the older sediments of Lake Suigetsu may also preserve a detailed record of Quaternary volcanism from Ulleungdo, which can permit a further understanding of the tempo and frequency of this volcanic centre.

In general, the Lake Suigetsu tephrostratigraphy suggests that an ash fall reached the central Honshu region at least once every 500 years throughout the Holocene. We suggest that these must have been at least VEI 4 events to be recorded as cryptotephra layers in Lake Suigetsu. It is clear that cryptotephra analysis in high-resolution distal archives can be used to provide additional information on these smaller eruption events that currently appear to be missing from the geological record (Kiyosugi *et al.*, 2015). These findings are of significant importance for risk assessments in East Asia. For instance, the 'International Atomic Energy Agency' require a detailed catalogue of past Holocene ash fall events to be compiled (e.g., eruption frequency, tephra thickness and direction of dispersal) before power plant construction is considered (Aspinall *et al.*, 2016).

7.3 Layers for synchronising palaeoenvironmental records

The most valuable tephra layers for palaeoenvironmental research are those which are i) regionally widespread, ii) possess a unique geochemical signature, iii) are precisely dated, and iv) occur at, or bracket a climate/cultural change. A key example from East Asia is the B-Tm ash, since it is identified across the Northern hemisphere (reaching Greenland; Sun *et al.*, 2014b), is precisely dated to AD 946 (Oppenheimer *et al.*, 2017; Hakozaik *et al.*, 2017) is

easily distinguished by its heterogeneous high-K composition, and occurs stratigraphically close to the onset of the Medieval Warm Period. The updated Holocene tephrostratigraphy from Lake Suigetsu indicates that there are several other widespread, geochemically unique, and now precisely dated isochrons that could be used to test and assess a range of questions relating to palaeoenvironmental change and drivers of the climate. For example, an abrupt cooling transition is known to have occurred ~ 8.2 ka yrs BP (widely known as the '8.2 event') via proxy records in Greenland (Figure 11) and across the North Atlantic region (see Alley *et al.*, 1997). The global synchronicity and duration of this event remains widely debated, however a similar abrupt cold event is dated to have occurred at 8.21 ± 0.05 kyr BP in China (Cheng *et al.*, 2009). The newly identified Changbaishan ash layer, dated to 8166 – 8099 cal. yrs BP (Figure 12), could therefore offer an important isochron to improve the chronology of palaeoclimate records in Japan, and assess any synchronous environmental changes during this time. It is therefore of significant importance to continue to search for ash layers in other palaeoenvironmental sites in the East Asian/Pacific region, which can permit a new perspective on such long-standing climate questions.

8. Conclusions

This study provides the first detailed Holocene cryptotephra study for the East Asian/Pacific region, and highlights the ability to identify distal ash layers in a productive arc setting.

Primary ash layers can be resolved even in lacustrine sediments that contain high concentrations of background glasses, if they contain distinctive shard morphologies and/or unique geochemical compositions. The Lake Suigetsu Holocene tephrostratigraphy provides the most comprehensive record to date of volcanism from East Asia, and is able to integrate twenty ash layers from a range of eruption magnitudes. As a result, these findings have now significantly extended the known ash dispersal of numerous key Holocene marker layers, including the Ma-b ash (Mashu), which is now identified over 1100 km from its source, and thus forms one of the most widely dispersed Japanese isochrons.

The Lake Suigetsu chronology is able to provide constrained eruption ages for all twenty ash layers, which offer a new insight into the frequency of explosive events from many of the volcanoes, including more precise repose intervals. These isochrons can now be robustly used to date and synchronise sedimentary records across Japan. Several of these stratigraphically constrain the onset and occurrence of rapid climate anomalies that occurred during the Holocene, and could provide a better understanding of climate drivers in this region. More work is required to robustly constrain the dispersal boundaries of these isochrons, with additional proximal glass geochemical datasets essential to testing future regional and hemispheric scale tephra correlations.

Acknowledgements

DM is funded by NERC (grant: NE/L002612/1) and part of the Environmental Research Doctoral Training Program at the University of Oxford. PGA and RAS are supported by Early Career Fellowships from the Leverhulme Trust (grant: ECF-2014-438 and ECF-2015-396). The Fukui-SG14 sediment coring campaign was funded by the Fukui Prefectural government, and the coring was conducted by the team of Seibushisui Co. Ltd. Japan, led by A. Kitamura. KAKENHI grant by MEXT, Japan (15H021443) was used to purchase laboratory equipment and consumables during the project. The authors would also like to thank M. Yamada for his assistance during the proximal sampling field campaign and two anonymous reviewers for their comments.

References

Abbott, P. M. and Davies, S. M. 2012. Volcanism and the Greenland ice-cores: the tephra record. *Earth-Science Reviews*, 115: 173-191

Abbott, P. M., Bourne, C. S., Purcell, C. S., Davies, S. M., Scourse, J. D. and Pearce, N. J. G. 2016. Last glacial period cryptotephra deposits in an eastern North Atlantic marine sequence: exploring linkages to the Greenland ice-cores. *Quaternary Geochronology*, 31: 62-76

Adhikari, D. P., Kumon, F. and Kawajiri, K. 2002. Holocene climate variability as deduced from the organic carbon and diatom records in the sediments of Lake Aoki, central Japan. *Jour. Geol. Soc. Japan*. 108: 249-265

Albert, P. G., Tomlinson, E. L., Smith, V. C., Di Roberto, A., Todman, A., Rosi, M., Marani, M., Muller, W. and Menzies, M. A. 2012. Marine-continental tephra correlations: volcanic glass geochemistry from the Marsili Basin and the Aeolian Islands, Southern Tyrrhenian Sea, Italy. *Journal of Volcanology and Geothermal Research*, 229: 74-94

Albert, P. G., Tomlinson, E. L., Lane, C. S., Wulf, S., Smith, V. C., Coltelli, M., Keller, J., Castro, D. L., Manning, C. J., Müller, W. and Menzies, M. A. 2013. Late glacial explosive activity on Mount Etna: Implications for proximal–distal tephra correlations and the synchronisation of Mediterranean archives. *Journal of Volcanology and Geothermal Research*, 265: 9-26

Albert, P. G., Hardiman, M., Keller, J., Tomlinson, E. L., Smith, V. C., Bourne, A. J., Wulf, S., Zanchetta, G., Sulpizio, R., Müller, U.C. and Pross, J. 2015. Revisiting the Y-3 tephrostratigraphic marker: a new diagnostic glass geochemistry, age estimate, and details on its climatostratigraphical context. *Quaternary Science Reviews*, 118: 105-121

Albert, P.G., Tomlinson, E.L., Smith, V.C., Di Traglia, F., Pistolesi, M., Morris, A., Donato, P., De Rosa, R., Sulpizio, R., Keller, J. and Rosi, M. 2017. Glass geochemistry of pyroclastic deposits from the Aeolian Islands in the last 50 ka: A proximal database for tephrochronology. *Journal of Volcanology and Geothermal Research*, 336: 81-107

Albert, P. G., Smith, V. C. Suzuki, T., Tomlinson, E., Nakagawa, T., Yamada, K., McLean, D., Staff, R. A., Schlolaut, G., Takemura, K., Nagahashi, Y., Kimura, I-P, SG06 Project Members. (submitted) Constraints on the frequency and dispersal of explosive eruptions at Sambe and Daisen volcanoes (South-West Japan Arc) from the distal Lake Suigetsu record (SG06 core). *Earth-Science Reviews*

Alley, R. B., Mayewski, P. A., Sowers, T., Stuiver, M., Taylor, K. C. and Clark, P. U. 1997. Holocene climatic instability: A prominent, widespread event 8200 yr ago. *Geology*, 25: 483-486

Alloway, B. V., Andreastuti, S., Setiawan, R., Miksic, J. and Hua, Q. 2017. Archaeological implications of a widespread 13th Century tephra marker across the central Indonesian Archipelago. *Quaternary Science Reviews*, 155: 86-99

Aoki, K., Irino, T., Oba, T. 2008. Late Pleistocene tephrostratigraphy of the sediment core MD01-2421 collected off the Kashima coast, Japan. *The Quat Res (Daiyonki-kenkyu)*, 47:391–407 (In Japanese with English abstract)

Aspinall, W. P., Charbonnier, S., Connor, C. B., Connor, L. J. C., Costa, A., Courtland, L. M., Delgado Granados, H., Godoy, A., Hibino, K., Hill, B. E. and Komorowski, J. C. 2016. *Volcanic Hazard Assessments for Nuclear Installations Methods and Examples in Site Evaluation* (No. 1795). International Atomic Energy Agency

Bacon, C. R. and Lanphere, M. A. 2006. Eruptive history and geochronology of Mount Mazama and the Crater Lake region, Oregon. *Geological Society of America Bulletin*, 118: 1331-1359

Barton, R. N. E., Lane, C. S., Albert, P. G., White, D., Collcutt, S. N., Bouzouggar, A., Ditchfield, P., Farr, L., Oh, A., Ottoloni, L., Smith, V. C., Van Peer, P. and Kindermann, K.,

2015. The role of cryptotephra in refining the chronology of Late Pleistocene human evolution and cultural change in North Africa. *Quaternary Science Reviews*, 118: 151-169

Blockley, S. P. E., Pyne-O'Donnell, S. D. F., Lowe, J. J., Matthews, I. P., Stone, A., Pollard, A. M., Turney, C. S. M. and Molyneux, E. G. 2005. A new and less destructive laboratory procedure for the physical separation of distal glass tephra shards from sediments. *Quaternary Science Reviews*, 24: 1952-1960

Bourne, A. J., Cook, E., Abbott, P. M., Seierstad, I. K., Steffensen, J. P., Svensson, A., Fischer, H., Schüpbach, S. and Davies, S. M. 2015. A tephra lattice for Greenland and a reconstruction of volcanic events spanning 25–45 ka b2k. *Quaternary Science Reviews*, 118: 122-141

Bourne, A., Abbott, P., Albert, P., Cook, E., Pearce, N., Ponomareva, V., Svensson, A. & Davies, S. 2016. Underestimated risks of recurrent long-range ash dispersal from northern Pacific Arc volcanoes. *Scientific Reports* 6, 29837

Bronk Ramsey, C. 2008. Deposition models for chronological records. *Quaternary Science Reviews*, 27: 42-60

Bronk Ramsey, C. 2017 OxCal Project, Version 4.3.
<https://c14.arch.ox.ac.uk/oxcal/OxCal.html> Retrieved June 2017

Bronk Ramsey, C., Staff, R. A., Bryant, C. L., Brock, F., Kitagawa, H., Van Der Plicht, J., Schlolaut, G., Marshall, M. H., Brauer, A., Lamb, H. F., Payne, R. L., Tarasov, P. E. Haraguchi, T., Gotanda, K., Yonenobu, H., Yokoyama, Y., Tada, R. and Nakagawa, T. 2012. A complete terrestrial radiocarbon record for 11.2 to 52.8 kyr BP. *Science*, 338: 370-374

Bussmann, F. and Anselmetti, F. S. 2010. Rossberg landslide history and flood chronology as recorded in Lake Lauerz sediments (Central Switzerland). *Swiss Journal of Geosciences*, 103: 43-59

Chen, X. Y., Blockley, S. P., Tarasov, P. E., Xu, Y. G., McLean, D., Tomlinson, E. L., Albert, P. G., Liu, J. Q., Müller, S., Wagner, M. and Menzies, M. A., 2016. Clarifying the distal to proximal tephrochronology of the Millennium (B–Tm) eruption, Changbaishan Volcano, northeast China. *Quaternary Geochronology*, 33: 61-75

Cheng, H., Fleitmann, D., Edwards, R. L., Wang, X., Cruz, F. W., Auler, A. S., Mangini, A., Wang, Y., Kong, X., Burns, S. J. and Matter, A. 2009. Timing and structure of the 8.2 kyr BP event inferred from $\delta^{18}\text{O}$ records of stalagmites from China, Oman, and Brazil. *Geology*, 37: 1007-1010

Chun, J. H., Cheong, D., Ikehara, K. and Han, S. J. 2007. Age of the SKP-I and SKP-II tephra from the southern East Sea/Japan Sea: implications for interstadial events recorded in sediment from marine isotope stages 3 and 4. *Palaeogeography, Palaeoclimatology, Palaeoecology*, 247: 100-114

Corella, J. P., Benito, G., Rodriguez-Lloveras, X., Brauer, A. and Valero-Garcés, B. L. 2014. Annually-resolved lake record of extreme hydro-meteorological events since AD 1347 in NE Iberian Peninsula. *Quaternary Science Reviews*, 93: 77-90

Davies, S. M., Elmquist, M., Bergman, J., Wohlfarth, B. and Hammarlund, D. 2007. Cryptotephra sedimentation processes within two lacustrine sequences from west central Sweden. *The Holocene*, 17: 319-330

Davies, S. M., Abbott, P. M., Meara, R. H., Pearce, N. J., Austin, W. E., Chapman, M. R., Svensson, A., Bigler, M., Rasmussen, T. L., Rasmussen, S. O. and Farmer, E. J., 2014. A North Atlantic tephrostratigraphical framework for 130–60 ka b2k: new tephra discoveries, marine-based correlations, and future challenges. *Quaternary Science Reviews*, 106: 101-121

Domitsu, H., Shiihara, M., Torii, M., Tsukawaki, S. and Oda, M., 2002. Tephrostratigraphy of

the piston cored sediment KT96-17 P-2 in the southern Japan Sea: the eruption age of Daisen-Kusadanihara Pumice (KsP). *Journal of the Geological Society of Japan*. 108: 545-556 (in Japanese with English abstract)

Fontijn, K., Rawson, H., Van Daele, M., Moernaut, J., Abarzúa, A. M., Heirman, K., Bertrand, S., Pyle, D. M., Mather, T. A., De Batist, M. and Naranjo, J.A., 2016. Synchronisation of sedimentary records using tephra: A postglacial tephrochronological model for the Chilean Lake District. *Quaternary Science Reviews*, 137: 234-254

Froggatt, P.C. 1983. Toward a comprehensive Upper Quaternary tephra and ignimbrite stratigraphy in New Zealand using electron microprobe analysis of glass shards. *Quaternary research*, 19: 188-200

Fujiwara, O., Sawa, Y., Morita, Y., Komatsubara, J. and Abe, K. 2007. Coseismic subsidence recorded in the Holocene sequence in the Ukishima-ka-hara, Shizuoka Prefecture, central Japan. *Annual Report on Active Fault and Paleoearthquake Researches*, 7: 91-118

Fukusawa, H. 1995. Non-glacial varved lake sediment as a natural timekeeper and detector on environmental changes. *The Quaternary Research (Daiyonki-kenkyu)*, 34: 135-149

Fukuoka, T. and Matsui, S., 2002. Stratigraphy of pyroclastic deposits post-dating the AT tephra, Sambe Volcano. *Earth Science (Chikyu Kagaku)*, 56: 105-122. (In Japanese with English abstract)

Furuta, T., Fujioka, K. and Arai, F. 1986. Widespread submarine tephra around Japan—petrographic and chemical properties. *Marine Geology*, 72: 125-142

Grant, K.M., Rohling, E.J., Bar-Matthews, M., Ayalon, A., Medina-Elizalde, M., Bronk Ramsey, C., Satow, C., and Roberts, A.P. 2012. Rapid coupling between ice volume and polar temperature over the past 150,000 years. *Nature*, 491: 744-747

- Gudmundsdóttir, E. R., Eiríksson, J. and Larsen, G. 2011. Identification and definition of primary and reworked tephra in Late Glacial and Holocene marine shelf sediments off North Iceland. *Journal of Quaternary Science*, 26: 589-602
- Hakozaki, M., Miyake, F., Nakamura, T., Kimura, K., Masuda, K. and Okuno, M. 2017. Verification of the Annual Dating of the 10th Century Baitoushan Volcano Eruption Based on an AD 774–775 Radiocarbon Spike. *Radiocarbon*, 1-8
- Hayakawa, Y. 1983. Chuseri tephra formation from Towada volcano, Japan. *Bull. Volcanol. Soc. Japan, Ser. 2*: 263-273
- Higashino, T., Tsujimori T. and Itaya T. 2005. An alkaline tephra found at Midagahara, Mt. Hakusan. 32. Ann Report Hakusan Nat Conserv Center 32: 1 –7
- Ikeya, N., Wada, H., Akutsu, H. and Takahashi, M. 1990. Origin and sedimentary history of Hamana-ko Bay, Pacific coast of central Japan. *Memoirs of the Geological Society of Japan: Lakes-Origin, Environment and Geology* 36: 129-150
- Ikehara, K., Danhara, T., Yamashita, T., Tanahashi, M., Morita, S. and Ohkushi, K. I. 2011. Paleooceanographic control on a large marine reservoir effect offshore of Tokai, south of Japan, NW Pacific, during the last glacial maximum-deglaciation. *Quaternary International*, 246: 213-221
- Im, J. H., Shim, S. H., Choo, C. O., Jang, Y. D. and Lee, J. S. 2012. Volcanological and palaeoenvironmental implication of charcoals of the Nari Formation in Nari Caldera, Ulleung Island, Korea. *Geosci. J*, 16: 105-114
- Ishimura, D., Yamada, K., Miyauchi, T. and Hayase, R. 2014. Characteristics of tephras interbedded with the Holocene sediments in the Sanriku Coast, northeast Japan. *J Geogra*, 123: 671-697

Jochum, K. P., Stoll, B., Herwig, K., Willbold, M., Hofmann, A. W., Amini, M. *et al.*, 2006. MPI-DING reference glasses for in situ microanalysis: New reference values for element concentrations and isotope ratios. *Geochemistry, Geophysics, Geosystems*, 7: 2

Karkanias, P., White, D., Lane, C. S., Stringer, C., Davies, W., Cullen, V. L., Smith, V. C., Ntinou, M., Tsartsidou, G. and Kyparissi-Apostolika, N. 2015. Tephra correlations and climatic events between the MIS6/5 transition and the beginning of MIS3 in Theopetra Cave, central Greece. *Quaternary Science Reviews*, 118: 170-181

Katsuta, N., Takano, M., Kawakami, S.I., Togami, S., Fukusawa, H., Kumazawa, M. and Yasuda, Y. 2007. Advanced micro-XRF method to separate sedimentary rhythms and event layers in sediments: its application to lacustrine sediment from Lake Suigetsu, Japan. *Journal of Paleolimnology*, 37: 259-271

Kim, G. B., Cronin, S. J., Yoon, W. S. and Sohn, Y. K. 2014. Post 19 ka BP eruptive history of Ulleung Island, Korea, inferred from an intra-caldera pyroclastic sequence. *Bulletin of Volcanology*, 76: 802

Kishimoto, H., Hasegawa, T., Nakagawa, M., Wada, K., 2009. Tephrostratigraphy and Eruption Style of Mashu Volcano, during the last 14,000 years, Eastern Hokkaido, Japan. *Bulletin of the Volcanological Society of Japan* 54, 15–36 (in Japanese with English abstract)

Kitagawa, H. and Van der Plicht, H. 1998a. A 40,000-year varve chronology from Lake Suigetsu, Japan: Extension of the C-14 calibration curve. *Radiocarbon*, 40: 505-515

Kitagawa, H. and Van der Plicht, H. 1998b. Atmospheric Radiocarbon Calibration to 45,000 yr B.P.: Late Glacial Fluctuations and Cosmogenic Isotope Production. *Science*, 279: 1187-1190

Kitagawa, H. and van der Plicht, J. 2000. Atmospheric radiocarbon calibration beyond 11,900 cal BP from Lake Suigetsu laminated sediments. *Radiocarbon*, 42: 370-381

Kitagawa, H., Fukuzawa, T. Nakamura, M., Okumura, K., Takemura, A., Hayashida, A. and Yasuda, Y. 1995. AMS ^{14}C dating of varved sediments from Lake Suigetsu, central Japan and atmospheric ^{14}C change during the late Pleistocene, *Radiocarbon*, 37: 371-378

Kiyosugi, K., Connor, C., Sparks, R.S.J., Crosweller, H.S., Brown, S.K., Siebert, L., Wang, T. and Takarada, S. 2015. How many explosive eruptions are missing from the geologic record? Analysis of the quaternary record of large magnitude explosive eruptions in Japan. *Journal of Applied Volcanology*, 4: 1-15

Kobayashi, M., Takada, A. and Nakano, S. 2007. Eruption history of Fuji Volcano from AD 700 to AD 1,000 using stratigraphic correlation of the Kouzushima-Tenjosan Tephra. *Bulletin of the Geological Survey of Japan*, 57: 409-430

Kumon, F., Kawai, S. and Inouchi, Y. 2003. Climate Changes between 25, 000 and 6, 000yrsBP Deduced from TOC, TN, and Fossil Pollen Analyses of a Sediment Core from Lake Nojiri, Central Japan. *The Quaternary Research (Daiyonki-Kenkyu)*, 42: 13-26

Lane, C. S., Brauer, A., Blockley, S. P. and Dulski, P. 2013. Volcanic ash reveals time-transgressive abrupt climate change during the Younger Dryas. *Geology*, 41: 1251-1254

Lane, C. S., Cullen, V. L., White, D., Bramham-Law, C. W. F. and Smith, V. C. 2014. Cryptotephra as a dating and correlation tool in archaeology. *Journal of Archaeological Science*, 42: 42-50

Lane, C. S., Brauer, A., Martín-Puertas, C., Blockley, S. P., Smith, V. C. and Tomlinson, E. L. 2015. The Late Quaternary tephrostratigraphy of annually laminated sediments from Meerfelder Maar, Germany. *Quaternary Science Reviews*, 122: 192-206

Le Bas, M. J., Le Maitre, R. W., Streckeisen, A. and Zanettin, B. 1986. A chemical classification of volcanic rocks based on the total alkali-silica diagram. *Journal of petrology*, 27: 745-750

Lim, C., Toyoda, K., Ikehara, K. and Peate, D.W. 2013. Late Quaternary tephrostratigraphy of Baegdusan and Ulleung volcanoes using marine sediments in the Japan Sea/East Sea. *Quaternary Research*, 80: 76-87

Lim, C., Kim, S. and Lee, C. 2014. Geochemical fingerprint of the primary magma composition in the marine tephras originated from the Baegdusan and Ulleung volcanoes. *Journal of Asian Earth Sciences*, 95: 266-273

Lowe, J., Barton, N., Blockley, S., Ramsey, C. B., Cullen, V. L., Davies, W., Gamble, C., Grant, K., Hardiman, M., Housley, R., Lane, C.S., Lee, S., Lewis, M., MacLeod, A., Menzies, M., Müller, W., Pollard, M., Price, C., Roberts, A. P., Rohling, E. J., Satow, C., Smith, V. C., Stringer, C. B., Tomlinson, E. L., White, D., Albert, P., Arienzo, I., Barker, G., Borić, D., Carandente, A., Civetta, L., Ferrier, C., Guadelli, J., Karkanias, P., Koumouzelis, M., Müller, U. C., Orsi, G., Pross, J., Rosi, M., Shalamanov-Korobar, L., Sirakov, N. and Tzedakis, P. C. 2012. Volcanic Ash Layers Illuminate the Resilience of Neanderthals and Early Modern Humans to Natural Hazards. *Proceedings of the National Academy of Sciences*, 109: 13532-13537

Lowe, J. J., Ramsey, C. B., Housley, R. A., Lane, C. S., Tomlinson, E. L., R.E.S.E.T. Team, R.E.S.E.T. Associates. 2015. The RESET project: constructing a European tephra lattice for refined synchronization of environmental and archaeological events during the last c. 100 ka. *Quaternary Science Reviews*, 118: 1-17

Mackay, H., Hughes, P. D., Jensen, B. J., Langdon, P.G., Pyne-O'Donnell, S. D., Plunkett, G., Froese, D. G., Coulter, S. and Gardner, J. E. 2016. A mid to late Holocene cryptotephra framework from eastern North America. *Quaternary Science Reviews*, 132: 101-113

Machida, H. and Arai, F. 1983. Extensive ash falls in and around the Sea of Japan from large late Quaternary eruptions. *Journal of Volcanology and Geothermal Research*, 18: 151-164

- Machida, H. and Arai, F. 2003. *Atlas of tephra in and around Japan*. Revised ed. Tokyo University Press, Tokyo
- Machida, H., Arai, F., Lee, B., Moriwaki, H. and Furuta, T. 1984. Late Quaternary tephras in Ulreung-do Island, Korea. *Journal of Geography (Chigaku-Zasshi)* 93: 1-14 (in Japanese with English abstract)
- Machida, H., H. Moriwaki, and D. Zhao. 1990. The recent major eruption of Changbai volcano and its environmental effects, *Geogr. Rep. Tokyo Metrop. Univ.*, 25: 1–20
- MacLeod, A. and Davies, S.M., 2016. Caution in cryptotephra correlation: resolving Lateglacial chemical controversies at Sluggan Bog, Northern Ireland. *Journal of Quaternary Science*, 31: 406-415
- Marshall, M., Schlolaut, G., Nakagawa, T., Lamb, H., Brauer, A., Staff, R., Ramsey, C.B., Tarasov, P., Gotanda, K., Haraguchi, T. and Yokoyama, Y. 2012. A novel approach to varve counting using μ XRF and X-radiography in combination with thin-section microscopy, applied to the Late Glacial chronology from Lake Suigetsu, Japan. *Quaternary Geochronology*, 13: 70-80
- Matsu'ura, T., Kimura, J. I., Chang, Q. and Komatsubara, J. 2017. Using tephrostratigraphy and cryptotephrostratigraphy to re-evaluate and improve the Middle Pleistocene age model for marine sequences in northeast Japan (Chikyu C9001C). *Quaternary Geochronology*, 40: 129-145
- McLean, D., Albert, P. G., Nakagawa, T., Staff, R. A., Suzuki, T. and Smith, V.C. 2016. Identification of the Changbaishan 'Millennium' (B-Tm) eruption deposit in the Lake Suigetsu (SG06) sedimentary archive, Japan: Synchronisation of hemispheric-wide palaeoclimate archives. *Quaternary Science Reviews*, 150: 301-307

- Moriwaki, H., Suzuki, T., Murata, M., Ikehara, M., Machida, H. and Lowe, D.J. 2011. Sakurajima-Satsuma (Sz-S) and Noike-Yumugi (N-Ym) tephras: new tephrochronological marker beds for the last deglaciation, southern Kyushu, Japan. *Quaternary International*, 246: 203-212
- Moriwaki, H., Nakamura, N., Nagasako, T., Lowe, D. J. and Sangawa, T., 2016. The role of tephras in developing a high-precision chronostratigraphy for palaeoenvironmental reconstruction and archaeology in southern Kyushu, Japan, since 30,000 cal. BP: An integration. *Quaternary International*, 397: 79-92
- Morrill, C., Overpeck, J.T. and Cole, J.E. 2003. A synthesis of abrupt changes in the Asian summer monsoon since the last deglaciation. *The Holocene*, 13: 465-476
- Nagahashi, Y., Yoshikawa, S., Miyakawa, C., Uchiyama, T. and Inouchi, Y. 2004. Stratigraphy and chronology of widespread tephra layers during the past 430 ky in the Kinki District and the Yatsugatake Mountains: major element composition of the glass shards using EDS analysis. *The Quaternary Research (Daiyonki-Kenkyu)* 43: 15-35 (in Japanese with English abstract)
- Nakagawa, M., Ishizuka, Y., Kudo, T., Yoshimoto, M., Hirose, W., Ishizaki, Y., Gouchi, N., Katsui, Y., Solovyov, A. W., Steinberg, G. S. and Abdurakhmanov, A. I. 2002. Tyatya volcano, southwestern Kuril arc: recent eruptive activity inferred from widespread tephra. *Island Arc*, 11: 236-254
- Nakagawa, T., Kitagawa, H., Yasuda, Y., Tarasov, P. E., Gotanda, K. and Sawai, Y. 2005. Pollen/event stratigraphy of the varved sediment of Lake Suigetsu, central Japan from 15,701 to 10,217 SG kyr BP (Suigetsu varve years before present): description, interpretation, and correlation with other regions. *Quaternary Science Reviews* 24: 1691–1701
- Nakagawa, T., Gotanda, K., Haraguchi, T., Danhara, T., Yonenobu, H., Brauer, A., Yokoyama, Y., Tada, R., Takemura, K., Staff, R. A., Payne, R., Bronk Ramsey, C., Bryant, C., Brock, F., Schlögl, G., Marshall, M., Tarasov, P., Lamb, H. and Suigetsu 2006 Project

- Members. 2012. SG06, a perfectly continuous and varved sediment core from Lake Suigetsu, Japan: stratigraphy and potential for improving the radiocarbon calibration model and understanding of late Quaternary climate changes. *Quaternary Science Reviews*, 36: 164-176
- Nakamura, Y. 2016. Stratigraphy, distribution, and petrographic properties of Holocene tephra in Hokkaido, northern Japan. *Quaternary International*, 397: 52-62
- Nakamura, Y., Nishimura, Y., Nakagawa, M., Kaistrenko, V. M., Iliev, A. Ya, 2009. Holocene marker tephra in the coastal lowlands of Kunashiri and Shikotan Islands, southern Kuril Islands. *Bulletin of the Volcanological Society of Japan (Kazan)* 54: 263-274 (in Japanese, with English abstract)
- Newhall, C. G. and Self, S. 1982. The volcanic explosivity index (VEI) an estimate of explosive magnitude for historical volcanism. *Journal of Geophysical Research: Oceans*, 87: 1231-1238
- Okuno, M., Shiihara, M., Torii, M., Nakamura, T., Kim, K. H., Domitsu, H., Moriwaki, H. and Oda, M. 2010. AMS radiocarbon dating of Holocene tephra layers on Ulleung Island, South Korea. *Radiocarbon*, 52: 1465-1470
- Okuno, M., Torii, M., Yamada, K., Shinozuka, Y., Danhara, T., Gotanda, K., Yonenobu, H. and Yasuda, Y. 2011. Widespread tephra in sediments from lake Ichi-no-Megata in northern Japan: Their description, correlation and significance. *Quaternary international*, 246: 270-277
- Oppenheimer, C., Wacker, L., Xu, J., Galván, J.D., Stoffel, M., Guillet, S., Corona, C., Sigl, M., Di Cosmo, N., Hajdas, I. and Pan, B., 2017. Multi-proxy dating the 'Millennium Eruption' of Changbaishan to late 946 CE. *Quaternary Science Reviews*, 158: 164-171
- Pan, B., de Silva, S.L., Xu, J., Chen, Z., Miggins, D.P. and Wei, H., 2017. The VEI-7 Millennium eruption, Changbaishan-Tianchi volcano, China/DPRK: New field, petrological, and chemical constraints on stratigraphy, volcanology, and magma dynamics. *Journal of Volcanology and Geothermal Research*.

- Park, M. H., Kim, I. S. and Shin, J. B. 2003. Characteristics of the late Quaternary tephra layers in the East/Japan Sea and their new occurrences in western Ulleung Basin sediments. *Marine Geology*, 202: 135-142
- Park, J. 2017. Solar and tropical ocean forcing of late-Holocene climate change in coastal East Asia. *Palaeogeography, Palaeoclimatology, Palaeoecology*, 469: 74-83
- Peccherillo, A. and Taylor, S.R. 1976. Geochemistry of Eocene calc-alkaline volcanic rocks from the Kastamonu area, northern Turkey. *Contributions to mineralogy and petrology*, 58: 63-81
- Pyne-O'Donnell, S. 2011. The taphonomy of Last Glacial–Interglacial Transition (LGIT) distal volcanic ash in small Scottish lakes. *Boreas*, 40: 131-145
- Ramos, F. C., Heizler, M. T., Buettner, J. E., Gill, J. B., Wei, H. Q., Dimond, C. A. and Scott, S. R. 2016. U-series and $^{40}\text{Ar}/^{39}\text{Ar}$ ages of Holocene volcanic rocks at Changbaishan volcano, China. *Geology*, 44: 511-514
- Reimer, P. J., Bard, E., Bayliss, A., Beck, J. W., Blackwell, P. G., Ramsey, C. B., Buck, C. E., Cheng, H., Edwards, R. L., Friedrich, M. and Grootes, P.M. 2013. IntCal13 and Marine13 radiocarbon age calibration curves 0–50,000 years cal BP. *Radiocarbon*, 55: 1869-1887
- Rohling, E. J., Grant, K., Bolshaw, M., Roberts, A. P., Siddall, M., Hemleben, C. and Kucera, M. 2009. Antarctic temperature and global sea level closely coupled over the past five glacial cycles. *Nature Geoscience*, 2: 500
- Sagawa, T., Kuwae, M., Tsuruoka, K., Nakamura, Y., Ikehara, M. and Murayama, M. 2014. Solar forcing of centennial-scale East Asian winter monsoon variability in the mid-to late Holocene. *Earth and Planetary Science Letters*, 395: 124-135

Saito-Kato, M., Yamada, K., Staff, R.A., Nakagawa, T., Yonenobu, H., Haraguchi, T., Takemura, K. and Bronk Ramsey, C. 2013. An assessment of the magnitude of the AD 1586 Tensho tsunami inferred from Lake Suigetsu sediment cores. *Journal of Geography (Chigaku Zasshi)* 122: 493-501 (in Japanese, with English abstract)

Sarna-Wojcicki, A. M., Morrison, S. D., Meyer, C. E. and Hillhouse, J. W. 1987. Correlation of upper Cenozoic tephra layers between sediments of the western United States and eastern Pacific Ocean and comparison with biostratigraphic and magnetostratigraphic age data. *Geological Society of America Bulletin*, 98: 207-223

Schlolaut, G., Marshall, M. H., Brauer, A., Nakagawa, T., Lamb, H. F., Staff, R. A., Bronk Ramsey, C., Bryant, C. L., Brock, F., Kossler, A., Tarasov, P. E., Yokoyama, Y., Tada, R. and Haraguchi, T. 2012. An automated method for varve interpolation and its application to the Late Glacial chronology from Lake Suigetsu, Japan. *Quaternary Geochronology*. 13: 52-69

Shane, P. 2000. Tephrochronology: a New Zealand case study. *Earth Science Reviews*, 49: 223-259

Shane, P., Sikes, E. L. and Guilderson, T. P. 2006. Tephra beds in deep-sea cores off northern New Zealand: implications for the history of Taupo Volcanic Zone, Mayor Island and White Island volcanoes. *Journal of Volcanology and Geothermal Research*, 154: 276-290

Shane, P. and Smith, I. 2000. Geochemical fingerprinting of basaltic tephra deposits in the Auckland Volcanic Field. *New Zealand Journal of Geology and Geophysics*, 43: 569-577

Shiihara, M., Torii, M., Okuno, M., Domitsu, H., Nakamura, T., Kim, K., Moriwaki, H. and Oda, M. 2011. Revised stratigraphy of Holocene tephra on Ulleung Island, South Korea, and possible correlatives for the U-Oki tephra. *Quaternary International* 246: 222-232

Shimada, S. 2000. Eruption of the Amagi-Kawagodaira Volcano and paleo- environments in the late and latest Jomon periods around Izu Peninsula. *The Quaternary Research (Daiyonki-Kenkyu)* 39: 151-164 (in Japanese with English abstract)

Shoji, S., Masui, J., 1974. ^{14}C age of Kamuinupuri volcanic ash soils in Shibecha, Kawakami country, Hokkaido ^{14}C age of the Quaternary deposits in Japan (97). *Earth Science (Chikyu Kagaku)* 28: 101 (in Japanese)

Smith, D. G. W. and Westgate, J. A. 1968. Electron probe technique for characterising pyroclastic deposits. *Earth and Planetary Science Letters*, 5: 313-319

Smith, V. C., Shane, P. and Nairn, I. A. 2005. Trends in rhyolite geochemistry, mineralogy, and magma storage during the last 50 kyr at Okataina and Taupo volcanic centres, Taupo Volcanic Zone, New Zealand. *Journal of Volcanology and Geothermal Research*, 148: 372-406

Smith, V. C., Pearce, N. J., Matthews, N. E., Westgate, J. A., Petraglia, M. D., Haslam, M., Lane, C. S., Korisettar, R. and Pal, J. N., 2011a. Geochemical fingerprinting of the widespread Toba tephra using biotite compositions. *Quaternary International*, 246: 97-104

Smith, V. C., Mark, D. F., Staff, R. A., Blockley, S. P. E., Bronk-Ramsey, C., Bryant, C. L., Nakagawa, T., Han, K. K., Weh, A., Takemura, K., Danhara, T. and Suigetsu 2006 Project Members. 2011b. Toward establishing precise Ar/Ar chronologies for Late Pleistocene palaeoclimate archives: an example from the Lake Suigetsu (Japan) sedimentary record, *Quaternary Science Reviews*, 30: 2845-2850

Smith, V. C., Staff, R. A., Blockley, S. P. E., Bronk Ramsey, C., Nakagawa, T., Mark, D. F., Takemura, K., Danhara, T. 2013. Identification and correlation of visible tephras in the Lake Suigetsu SG06 sedimentary archive, Japan: Chronostratigraphic markers for synchronising of east Asian/west Pacific Pacific palaeoclimatic records for 150ka, *Quaternary Science Reviews*, 61: 121-137

Staff, R. A., Bronk Ramsey, C., Bryant, C. L., Brock, F., Payne, R. L., Schlolaut, G., Marshall, M. H., Brauer, A., Lamb, H. F., Tarasov, P., Yokoyama, Y., Haraguchi, T., Gotanda, K., Yonenobu, H., Nakagawa, T. and Suigetsu 2006 project members. 2011. New ^{14}C determinations from Lake Suigetsu, Japan: 12,000 to 0 cal bp, *Radiocarbon*, 53: 511-528

Staff, R. A., Schlolaut, G., Ramsey, C. B., Brock, F., Bryant, C. L., Kitagawa, H., Van der Plicht, J., Marshall, M. H., Brauer, A., Lamb, H. F. and Payne, R. L. 2013a. Integration of the old and new Lake Suigetsu (Japan) terrestrial radiocarbon calibration data sets. *Radiocarbon*, 55: 2049-2058

Staff, R. A., Nakagawa, T., Schlolaut, G., Marshall, M.H., Brauer, A., Lamb, H. F., Bronk Ramsey, C., Bryant, C. L., Brock, F., Kitagawa, H. and Plicht, J., 2013b. The multiple chronological techniques applied to the Lake Suigetsu SG06 sediment core, central Japan. *Boreas*, 42: 259-266.

Sun, C., Plunkett, G., Liu, J., Zhao, H., Sigl, M., McConnell, J. R., Pilcher, J. R., Vinther, B., Steffensen, J. P. and Hall, V. 2014a. Ash from Changbaishan Millennium eruption recorded in Greenland ice: Implications for determining the eruptions timing and impact. *Geophysical Research Letters*, 41: 694-701

Sun, C., You, H., Liu, J., Li, X., Gao, J. and Chen, S. 2014b. Distribution, geochemistry and age of the Millennium eruptives of Changbaishan volcano, Northeast China—A review. *Frontiers of Earth Science*, 8: 216-230

Sun, C., You, H., He, H., Zhang, L., Gao, J., Guo, W., Chen, S., Mao, Q., Liu, Q., Chu, G. and Liu, J., 2015. New evidence for the presence of Changbaishan Millennium eruption ash in the Longgang volcanic field, Northeast China. *Gondwana Research*, 28: 52-60

Sugiuchi, Y. and Kukuoka, T. 2005. Tephrochronology of recent (~1200 YBP) Mt. Fuji eruption history using rhyolitic tephra derived from outside Mt. Fuji Volcano, *International Field Conference and Workshop on Tephrochronology and Volcanism: "Tephra Rush 2005"*, INQUA Sub-Commission for Tephrochronology and Volcanism (SCOTAV)

Suzuki, Y., Tada, R., Yamada, K., Irino, T., Nagashima, K., Nakagawa, T. and Omori, T. 2016. Mass accumulation rate of detrital materials in Lake Suigetsu as a potential proxy for

heavy precipitation: a comparison of the observational precipitation and sedimentary record.

Progress in Earth and Planetary Science, 3: 5

Suzuki, T., Nishizawa, F., Ishimura, D. Ito, M., Maruyama, S., Danhara, T. and Hirata, T. 2017. Re-examination of identification and discrimination of Kozu-Tenjosan and Nijima-Mukaiyama tephras, Izu Islands, Japan. Japan Association for Quaternary Research, Programme and Abstracts, 47: 49 (In Japanese)

Swierczynski, T., Brauer, A., Lauterbach, S., Martín-Puertas, C., Dulski, P., von Grafenstein, U. and Rohr, C. 2012. A 1600 yr seasonally resolved record of decadal-scale flood variability from the Austrian Pre-Alps. *Geology*, 40: 1047-1050

Tada, R. and Murray, R.W. 2016. Preface for the article collection “Land–Ocean Linkages under the Influence of the Asian Monsoon”. *Progress in Earth and Planetary Science*, 3: 24

Tani, S., Kitagawa, H., Hong, W., Park, J. H., Sung, K. and Park, G. 2013. Age determination of the Kawagodaira volcanic eruption in Japan by ¹⁴C wiggle-matching. *Radiocarbon*, 55: 748-52

Takemura, K., Iwabe, C., Hayashida, A., Danhara, T., Kitagawa, H., Haraguchi, T., Sato, T., Ishikawa, N. 2010. Stratigraphy of marker tephras and sediments during the past 50,000 years from multiple sites in Lake Biwa, Japan. *Quaternary Research* 49: 147–60 (In Japanese with English abstract)

Tomlinson, E. L., Smith, V. C., Albert, P. G., Aydar, E., Civetta, L., Cioni, R., Çubukçu, E., Gertisser, R., Isaia, R., Menzies, M. A. and Orsi, G. 2015. The major and trace element glass compositions of the productive Mediterranean volcanic sources: tools for correlating distal tephra layers in and around Europe. *Quaternary Science Reviews*, 118: 48-66

Turney, C.S., 1998. Extraction of rhyolitic component of Vedde microtephra from minerogenic lake sediments. *Journal of Paleolimnology*, 19: 199-206

Tsuchiya, M., Mannen, K., Kobayashi, M. and Fukuoka, T. 2017. Two types of glass shards within the Owakidani tephra group deposit, Hakone Volcano: Constraints on their sources and ages, 62: 23-30 (in Japanese with English abstract)

Tsukui, M., Saito, K. and Hayashi, K. 2006. Frequent and intensive eruptions in the 9th century, Izu Islands, Japan: Revision of volcano-stratigraphy based on tephra and historical document. *Bulletin of Volcanological Society of Japan*, 1: 327-338

Walker, M., Johnsen, S., Rasmussen, S.O., Popp, T., Steffensen, J.P., Gibbard, P., Hoek, W., Lowe, J., Andrews, J., Björck, S. and Cwynar, L.C. 2009. Formal definition and dating of the GSSP (Global Stratotype Section and Point) for the base of the Holocene using the Greenland NGRIP ice core, and selected auxiliary records. *Journal of Quaternary Science*, 24: 3-17

Wada, K., Nakamura, M. and Okuno, M., 2001. Identification of source volcano from the chemical compositions of glasses from the widespread ashes in the surface layers of Asahidake volcano, Central Hokkaido, Japan. *Reports of the Taisetsuzan Institute of Science*, 35: 9-18

Wang, Y., Cheng, H., Edwards, R. L., He, Y., Kong, X., An, Z., Wu, J., Kelly, M. J., Dykoski, C.A. and Li, X. 2005. The Holocene Asian monsoon: links to solar changes and North Atlantic climate. *Science*, 308: 854-857

Wanner, H., Beer, J., Bütikofer, J., Crowley, T.J., Cubasch, U., Flückiger, J., Goosse, H., Grosjean, M., Joos, F., Kaplan, J.O. and Küttel, M., 2008. Mid-to Late Holocene climate change: an overview. *Quaternary Science Reviews*, 27: 1791-1828

Wastegård, S., 2002. Early to middle Holocene silicic tephra horizons from the Katla volcanic system, Iceland: new results from the Faroe Islands. *Journal of Quaternary Science*, 17: 723-730

Watkins, N. D., Sparks, R. S. J., Sigurdsson, H., Huang, T. C., Federman, A., Carey, S. and Ninkovich, D. 1978. Volume and extent of the Minoan tephra from Santorini Volcano: new evidence from deep-sea sediment cores. *Nature*, 271: 122-6

Wei, H., Sparks, R. S. J., Liu, R., Fan, Q., Wang, Y., Hong, H., Zhang, H., Chen, H., Jiang, C., Dong, J. and Zheng, Y., 2003. Three active volcanoes in China and their hazards. *Journal of Asian Earth Sciences*, 21: 515-526

Xu, J., Liu, G., Wu, J., Ming, Y., Wang, Q., Cui, D., Shangguan, Z., Pan, B., Lin, X. and Liu, J. 2012. Recent unrest of Changbaishan volcano, northeast China: A precursor of a future eruption? *Geophysical Research Letters*, 39: 16

Yamada, K., Takemura, K., Kuwae, M., Ikehara, K. and Yamamoto, M. 2016. Basin filling related to the Philippine Sea Plate motion in Beppu Bay, southwest Japan. *Journal of Asian Earth Sciences*, 117: 13-22

Yamada, K., Nakagawa, T., Staff, R., Kitaba, I., Kitagawa, J., McLean, D., Smith, V., Haraguchi, Albert, P., Suzuki, Y., Gotanda, K., Hyodo, M. and Takemura, K. Submitted. Stratigraphy and sedimentation rate changes of the Lake Suigetsu (SG14) core, Fukui Prefecture, central Japan

Zawalna-Geer, A., Lindsay, J.M., Davies, S., Augustinus, P. and Davies, S. 2016. Extracting a primary Holocene cryptotephra record from Pupuke maar sediments, Auckland, New Zealand. *Journal of Quaternary Science*, 31: 442-457